

1. Project No. SWUTC/11/161106-1		2. Government Accession No.		3. Recipient's Catalog No.	
4. Title and Subtitle Evaluating the Effect of Street Network Connectivity on First/Last Mile Transit Performance				5. Report Date November 2011	
				6. Performing Organization Code	
7. Author(s) Luca Quadrifoglio and Shailesh Chandra				8. Performing Organization Report No.	
9. Performing Organization Name and Address Texas Transportation Institute The Texas A&M University System 3135 TAMU College Station, TX 77843-3135				10. Work Unit No. (TRAIS)	
				11. Contract or Grant No. 10727	
12. Sponsoring Agency Name and Address Southwest Region University Transportation Center Texas Transportation Institute Texas A&M University System College Station, Texas 77843-3135				13. Type of Report and Period Covered	
				14. Sponsoring Agency Code	
15. Supplementary Notes Supported by general revenues from the State of Texas.					
16. Abstract This study defines a novel connectivity indicator (CI) to predict transit performance by identifying the role that street network connectivity plays in influencing the service quality of demand responsive feeder transit services. This new CI definition is dependent upon the expected shortest path between any two nodes in the network, includes spatial features and transit demand distribution information, and is easy to calculate for any given service area. Simulation analyses over a range of networks are conducted to validate the new definition. Results show a desirable monotonic relationship between transit performance and the proposed CI, whose values are directly proportional and therefore good predictors of the transit performance, outperforming other available indicators typically used by planners. This study also presents a methodology to identify and locate critical links in a grid street network system of any size for feeder transit services. A critical link can be defined as that link that when eliminated from or appended to an existing network would cause the largest change in the network connectivity and consequently transit performance. Easily computable formulas are provided and validated by simulation analyses. Useful insights indicate a monotonic decrease in link criticality as we depart from the centrally located links to those located at boundaries.					
17. Key Word First/Last Mile, Demand Responsive, Connectivity, Critical Link, Insertion Heuristic			18. Distribution Statement No restrictions. This document is available to the public through NTIS: National Technical Information Service 5285 Port Royal Road Springfield, Virginia 22161		
19. Security Classif. (of this report) Unclassified		20. Security Classif. (of this page) Unclassified		21. No. of Pages 64	22. Price

Evaluating the Effect of Street Network Connectivity on First/Last Mile Transit Performance

by
Luca Quadrioglio
Shailesh Chandra

Research Report SWUTC/11/161106-1

Texas Transportation Institute
The Texas A&M University System
3135 TAMU
College Station, TX 77843-3135

November 2011

DISCLAIMER

The contents of this report reflect the views of the authors, who are responsible for the facts and the accuracy of the information presented herein. This document is disseminated under the sponsorship of the Department of Transportation, University Transportation Centers Program, in the interest of information exchange. Mention of trade names or commercial products does not constitute endorsement or recommendation for use.

ACKNOWLEDGMENTS

The authors recognize that support for this research was provided by a grant from the U.S. Department of Transportation, University Transportation Centers Program to the Southwest Region University Transportation Center, which is funded, in part, with general revenue funds from the State of Texas.

EXECUTIVE SUMMARY

Feeder transit services provide the ultimate first/last mile access for passengers, and their performance is intuitively dependent upon the street network design and its connectivity, as vehicles are potentially required to reach any point in the service area to serve the demand. The higher the network connectivity is, the faster and more efficiently vehicles are able to serve customers, and the better the feeder transit service can perform. Having information that is more informative and detailed regarding the relationship between the road network design (and its connectivity) and the expected transit performance would be very desirable for properly planning the development of residential areas with the goal of enhancing their transportation mobility. However, this correlation has yet to be scientifically investigated, and it is not trivially computed. The purpose of this study is to perform a quantification of it.

Public transportation is in constant competition with private vehicles for providing mobility to the general public. Its well-known lesser convenience, flexibility, and connectivity are emphasized by the progressive increase of urban sprawl, making it harder and harder for public transportation to be attractive to customers. With state and local revenues declining due to the recession, public transit systems are in addition facing severe financial challenges. As America struggles to create jobs, rising fares and cuts in service drive people away from using public transit. Most modes of public transportation have in fact seen a decline in ridership during the last years [1].

The Department of Transportation recently identified the general lack of connectivity as one of the main challenges faced by public transit. Policies that encourage the desired reduction of vehicle miles traveled (VMT), reduction of greenhouse gases, and increase of livability depend on solutions to the issue of first/last mile access to transit and multimodal connectivity. Public transportation must continue to explore and evaluate innovative ways of providing safe, convenient, and efficient public transportation options to properly address the issue. One of the possible solutions to this problem is the planning, design, and implementation of efficient demand responsive door-to-door feeder transit services.

A public transit service relies heavily on an efficient scheduling operation of its fleet. Scheduling operations usually need an idea of the route the bus or shuttle is going to follow, which in turn is dependent on the degree of connectivity the street system has. A large portion of

the trip performance for transit buses, whether flexible or fixed in nature, depends on their ability to move fast between two demand points on a link. Generally and intuitively, the shorter the distance, the faster the journey and the higher the performance. This is particularly true for demand responsive types of services, which might need to use a much larger portion of the network links due to the random nature of their routes. One-way street systems and turn bays at intersections restrict ease of movement of the bus/shuttle by lowering its speed in certain parts of the street network. Degree of congestion on a network link also plays a role in influencing the point-to-point travel time. Congestion, in turn, is dependent on varieties of factors, such as the presence of traffic control devices, parking provisions, incidents, maintenance activities, etc. All these factors affect travel time of a vehicle in the network system. A good connectivity would thus mean accessibility of points on the street network with minimum travel time. Therefore, it is obvious that a minimized travel time leads to an improved transit performance and ultimately complete customer satisfaction.

In this study, we focus on demand responsive transit (DRT) services, which are mostly used for residential first/last mile operations. The feeder DRT service could be defined as one vehicle operating continuously during the day. The vehicle starts from the terminal every h minutes to serve customers door to terminal and terminal to door in a shared-ride fashion. Scheduling must be performed wisely in order to be able to come back to the terminal after h minutes of operations. To perform the scheduling operation, Dijkstra's algorithm is employed to calculate the shortest paths between each pair of demand points; an insertion heuristic algorithm is adopted to calculate the actual schedule of the vehicle. A proper use of sparse matrix is employed to perform these computational tasks more efficiently.

A good street network model is also judged by the effects it has on the performance of DRT systems, should future urban planners consider transit a necessary (if not mandatory) service as a part of the livability of communities. This research is a step toward studying the effects of denser and sparser street networks on DRT shuttle performance. Street connectivity studies are also useful in implementation of traffic plans that reduce vehicle miles traveled, and schemes that exist at the present time do not precisely link performance measures of a transit with respect to street network design.

This study identifies and tests a new connectivity indicator that is simple to define, easy to compute, and able to properly capture the relationship between DRT performance and street

network connectivity. Further, this study also explores the methodology for identification of critical links in a network system from a DRT performance point of view with some closed-form results that will help planners and engineers decide on the most critical link without involving exhaustive computations or simulations. Critical links of a grid-based network are identified as those that when removed/closed would cause the largest drop in the DRT shuttle performance. Simulation experiments are performed to validate the critical link(s) determined analytically. Useful insights indicate a monotonic decrease in link criticality as we depart from the centrally located links to those located at boundaries.

TABLE OF CONTENTS

CHAPTER 1. INTRODUCTION.....	1
CHAPTER 2. BACKGROUND AND LITERATURE REVIEW.....	5
CHAPTER 3. STREET CONNECTIVITY FRAMEWORK.....	9
3.1 CONNECTIVITY INDICATOR.....	10
3.2 PERFECT CONNECTIVITY FOR STREET NETWORKS.....	12
3.2.1 AVERAGE CLOSEST STREET-BASED DISTANCE.....	15
CHAPTER 4. STREET NETWORK MODELING.....	19
CHAPTER 5. SIMULATION EXPERIMENTS.....	25
5.1 TESTING NEW CONNECTIVITY INDICATOR.....	25
5.1.1 SIMULATION INPUT—PASSENGER REQUEST TIMES.....	26
5.1.2 STREET NETWORK SYSTEM DESCRIPTION.....	28
5.1.3 NUMERICAL CALCULATIONS OF CONNECTIVITY INDICES/ INDICATORS.....	31
5.1.4 CONNECTIVITY INDICATOR—SIMULATION RESULTS AND DISCUSSIONS.....	33
5.2 SIMULATION TESTING FOR CRITICAL LINKS.....	38
CHAPTER 6. CONCLUSIONS.....	41
REFERENCES.....	43
APPENDIX.....	49

LIST OF FIGURES

FIGURE 1: Evolution of street patterns.	5
FIGURE 2: On-demand bus-stop nodes on cross-street links.	10
FIGURE 3: A grid section of the street network system of the town of Hempstead, TX (Source: Google Earth).	13
FIGURE 4: A perfect street network system.	14
FIGURE 5: Locating the closest on-demand node from a known node Z	16
FIGURE 6: Removal of a link to create a new network from an old network.	20
FIGURE 7: Grid street system of Hempstead, TX (Source: Google Maps).	20
FIGURE 8: Variation of Δd along the cross-section of the street network.	24
FIGURE 9: Cumulative density function for U.S. work trips for departure and arrival (arrival starts at 2 p.m.).	27
FIGURE 10: Examples of existing street patterns.	30
FIGURE 11: Variation of U versus different connectivity indicator values.	34
FIGURE 12: Different street systems within network (6).	36
FIGURE 13: Disutility versus connectivity index variation for different demand distributions.	37
FIGURE 14: Sequential link closures/removals 1-2-3-4-5 to create five different sets of street networks.	38
FIGURE 15: Performance effects on DRT for the sequential link closures/removals.	40
FIGURE 16: Sketch depicting the target node in the street network system.	49
FIGURE 17: Split regions to create target node for any intermediate node.	51
FIGURE 18: Enclosed nodes for computing $R_{(x,y)}$	52

LIST OF TABLES

Table 1: Simulation Inputs for Connectivity Indicator.	25
Table 2: Connectivity Index/Indicator Evaluated for the Five Networks.	32
Table 3: Disutility Output Values for Different Networks.	33

CHAPTER 1. INTRODUCTION

Public transportation is in constant competition with private vehicles for providing mobility to the general public and has seen a decline in ridership during the last decades [1]. The U.S. Department of Transportation recently identified the general lack of connectivity as one of the main reasons for the decline. This lack is in addition to public transportation's well-known lesser convenience and reduced flexibility, which is emphasized by the progressive increase of urban sprawl, making it harder and harder for public transit to be attractive to customers. Policies that encourage the desired reduction of vehicle miles traveled (VMT), reduction of greenhouse gases, and increase of "livability" depend on solutions to the issue of first/last mile access to transit and multimodal solutions. Thus, public transportation must continue to explore and evaluate innovative ways of providing safe, convenient, and efficient public transportation options to properly address the issue.

The primary purpose of a street network system is to connect spatially separated places and provide movement from one place to another. The nature of these connections varies depending on the structure and design of the street network system, from being one to many, direct to indirect, or even divided among the kinds of connections to support different modes of travel. Qualitatively, these connections are expressed as the "connectivity" of the street network and influence the accessibility of potential destinations in a community. Connectivity has important implications, as its quality influences the efficiency of public transportation, travel choices, and emergency access and adds to the livability of a community.

Feeder transit services provide the ultimate first/last mile access for passengers, and their performance is intuitively dependent upon the street network design and its connectivity, as vehicles are potentially required to reach any point in the service area to serve the demand. The

higher the network connectivity, the faster and more efficiently vehicles are able to serve customers and the better the feeder transit service can perform. Having information that is more informative and detailed regarding the relationship between the street network design (and its connectivity) and the expected transit performance would be very desirable for properly planning the development of residential areas with the goal of enhancing their transportation mobility. However, this correlation has yet to be scientifically investigated, and it is not trivially computed. Current connectivity measures are not sufficiently accurate or linked to transit performance, as will be shown later in this study.

Transportation networks play a very important role in providing timely access for travelers in the form of connectivity between the origins and destinations. It is essential that every element of a transportation network function properly for an efficient movement of traffic. Every individual street link functions differently depending on its capability to facilitate smooth vehicular traffic flow. Traffic flow is often obstructed due to the presence of intersections and various other traffic-calming devices. However, over a given street network system, vehicular traffic as a whole can be coordinated to avoid congestion situations that eventually lead to concentrated traffic on one street link and completely absent vehicular traffic on others. This is easily achieved by uniformly distributing traffic over the street systems, resulting in good street connectivity that provides multiple driving options. However, in the real world, some links are always favored for traveling, simply because of a higher speed option that they have over other links. This eventually gives rise to an uneven distribution of traffic over the network and, as a result, often burdens certain links beyond their capacity. Sometimes, absence of an alternative route also forces traffic to pile up on these links, thereby making them more vital and critical than other links. This calls for keeping a close watch and scheduling maintenance activities on a regular basis on these links. Closure of these links due to incidents or heavy congestion could

impact the average vehicle performance on the street system in terms of greenhouse gas emissions and unwanted driving times or waiting times in traffic. Studying these links becomes even more essential when they lie on a major transit line such as a bus route, as its failure would affect a large number of commuters. Thus, it becomes important to understand the location of those links that could be critical for commuting.

Advance knowledge of the location of critical links in a network can be vital for assisting transit operators to re-route the path traversed by shuttles or buses appropriately so that minimal delay is caused to the riders when that critical link along its route fails. Transit buses that follow a flexible routing strategy during passenger pick-up/drop-off have more freedom in this regard than the transit buses that operate over a fixed route and fixed number of stops. In this light, thus, feeder demand responsive transit (DRT), which is completely flexible in its service, would benefit the most from having advance knowledge of critical links in a network it uses.

Demand responsive transport or demand responsive transit is characterized by a flexible routing and scheduling of a bus/shuttle operating in shared-ride mode between pick-up and drop-off locations according to passengers' needs. In many areas, DRT is instead known as DART, or Dial-a-Ride Transit [2]. DRT systems provide a convenient public transport service in areas of low passenger demand. Usually, DRT schemes are fully or partially funded by the local transit authority in the form of socially necessary transport. At other times, DRT service is provided by private operators. As far as the operability of the DRT is concerned, the main aim of the operators is to ensure best service standards for the passengers. A prior knowledge of critical links can be of immense help to the DRT operators, who can easily re-route a bus's traversed path to avoid a failed link in a network and yet cause minimal or no delay to passengers that it serves.

From the above discussions, it is easy to see that the performance indicators of the DRT services are dependent on the street network topology. A good street connectivity is important for both the travelers and the transit operators. Measures are needed to assess the robustness of this network connectivity in case of link failures due to a variety of plausible scenarios, such as planned maintenance, accidents, or emergency evacuations for terrorist attacks or flooding. However, quantifying the criticality of the links in a given network for transit performance is not trivial. The purpose of this study is to identify and test a new connectivity indicator (CI) that is simply defined, easily computable, and able to properly capture the relationship between DRT performance and street network connectivity. Further, this study also explores the methodology for identification of critical links in a network system from a DRT performance point of view with some closed-form results that will help planners and engineers decide on the most critical link without involving exhaustive computations or simulations. Critical links of a grid-based network are identified as those that when removed/closed would cause the largest drop in the DRT shuttle performance. Simulation experiments are performed to validate the critical links determined analytically.

CHAPTER 2. BACKGROUND AND LITERATURE REVIEW

Early 19th century street network systems in residential areas were characterized by a grid pattern considered to be suitable for pedestrian as well as vehicle movements. With a gradual increase in automobile use, these street patterns gave way to curvilinear street network systems. The images in Fig. 1 show the gradual evolution of street network systems [3].

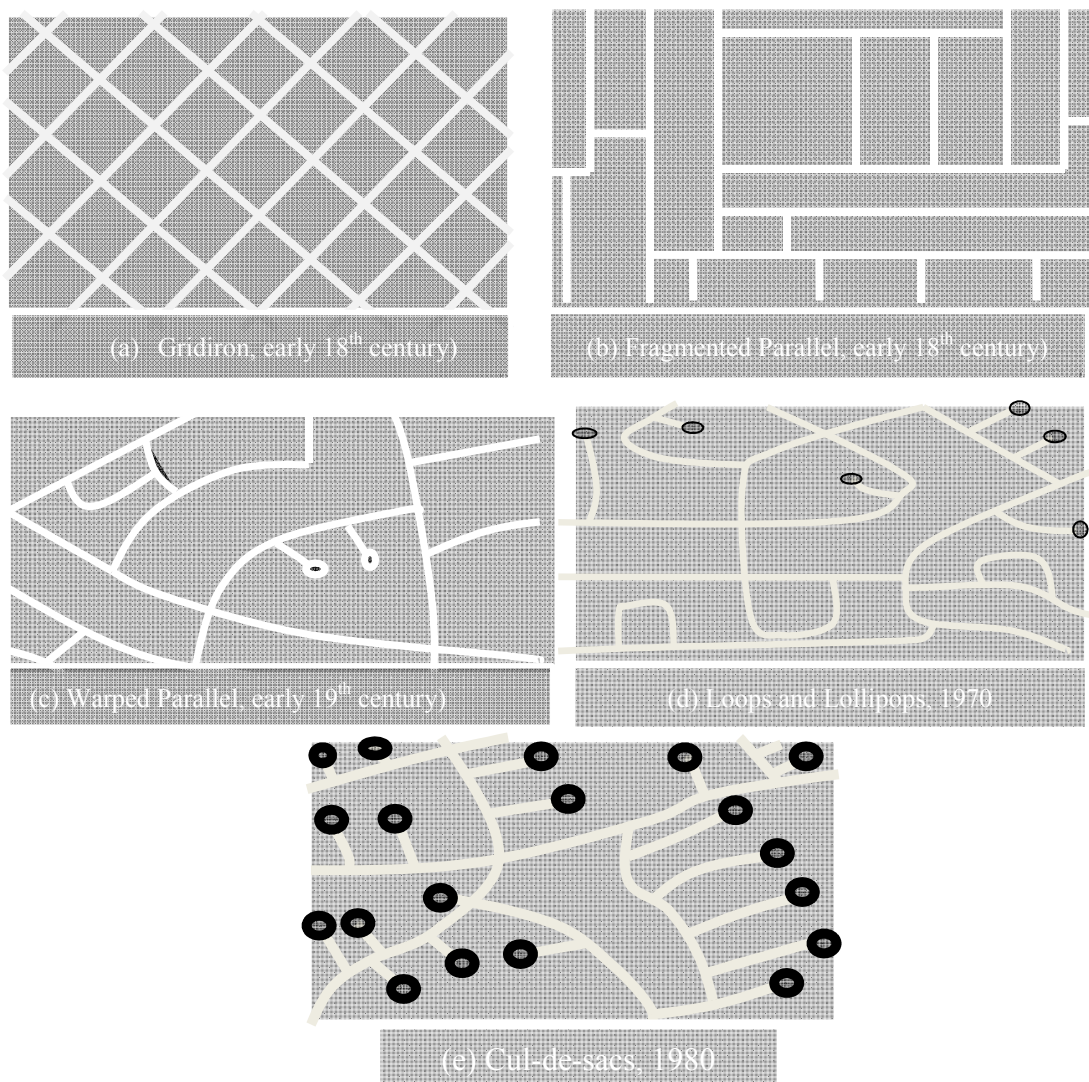


FIGURE 1: Evolution of street patterns.

By the 1980s, most of the planning aimed at separating the residential subdivisions from the vehicular road network through the introduction of cul-de-sac kinds of street patterns [3]. Cul-de-sacs or dead ends not only serve as a barrier to the pedestrian movements across the streets but also delay and obstruct vehicle navigation. As the need for better connectivity has lately grown among planners and engineers, particularly within residential areas, there is an increasing advocacy by city transport officials to revert to promoting the grid network kind of street structure back in place across the U.S. The State of Virginia, for example, has already outlawed cul-de-sac types of street system design [4].

There are a number of attempts from researchers and practitioners to identify a good way to properly measure street connectivity with connectivity indices or indicators. Block length, block size, and block densities are used as some of the ways to measure street connectivity ([5], [6], [7]). However, the requirements for the block length, size, or density are restricted to only pedestrian and bicycle connections. Planners extensively use a connectivity index, defined as the ratio of the number of links (usually defined as the segment between two nodes or intersections) to the number of intersections ([4],[8]), but the connectivity index defined using this ratio does not incorporate the link length information, which intuitively affects connectivity. It is also quite easy to visualize that with the same connectivity index definition above, two different streets could have the same connectivity index values depending on the way street link segments are counted [9].

Peponis et al. (2007, 2008) introduced the concepts of “reach” and “directional distance” as the measures of connectivity applicable to geographic information system (GIS)-based representations of street networks. However, this measure of connectivity lacks a closed-form expression for defining the connectivity index for any general network ([10], [11]). The Gamma index that exists in Kansky (1963) is particularly useful in quantifying connectivity for a

particular street network but does not include provisions for ridership demands or any passenger utility [12].

Derrible and Kennedy (2009, 2010a, 2010b) studied the metro transit network system as graphs, and in some sense, there was a link between the connectivity and transit performance ([13], [14], [15]). However, metro rails have fixed tracks that they follow as a travel constraint and, hence, do not bear very close resemblance to flexibility of other modes of transit (such as DRT), which use streets.

A vehicle's performance estimation with respect to a street network's connectivity index is particularly important for designing mass transit systems, especially when there is a choice between two street networks. Since there is a considerable monetary investment that is involved in setting up a transit system for an unknown area, considering connectivity indices of the two street networks could help transportation planners in deciding on one of the street networks for best transit performance.

It is generally difficult to identify a unique definition of performance of a transit system, as priorities differ among stakeholders. Several authors have used measures such as passenger cost, passengers per vehicle hour, vehicle miles per operator, cost per vehicle mile, cost per vehicle hour, ratio of cost to fare box revenue, and fleet fuel efficiency for the urban public transit ([16],[17],[18],[19]). However, all seem to agree that transit performance can generally be identified as a combination of operating costs and service quality. The service quality is expressed as passengers' disutility: a weighted sum of expected waiting time, expected in-vehicle travel time, and walking time for using the DRT service [20].

Literature on single link failures exists where an increase in travel time or travel distance for the commuters has been considered as a vital component in the determination of critical links. Jenelius et al. (2006) derived several link importance indices and site exposure indices based on

the increase in generalized travel cost when links are closed [21]. The measures used were divided into two groups—the first one reflected an “equal opportunities perspective” and the second a “social efficiency perspective.” These measures were calculated for the road network of northern Sweden. Knoop et al. (2007) developed many indicators to determine vulnerable parts of a network [22]. These were determined without simulating the network flows with an incident on each of the links. Further, a list of indicators was proposed in the literature and comparisons were made. It was observed that different indicators ranked links differently.

Taylor et al. (2006) performed a vulnerability analysis on road networks by considering the socioeconomic impacts of network degradation [23]. Several standard indices of accessibility were considered, which included a generalized travel cost, the Hansen integral accessibility index, and the Accessibility/Remoteness Index of Australia (ARIA) index used in Australia.

However, the evaluation is not explicitly based on the impacts on vehicular performances for any given link’s failure. Often, a solvable approximation is needed for identifying the most vital arc or link in a network using some algorithmic approach. Ball and Golden (1989) used the most vital arcs problem (MVAP) to find a subset of arcs whose removal from the network resulted in the greatest increase in the shortest distance between two specified nodes [24]. Corley and Sha (1982) used algorithms to identify the most vital links (or nodes) in a weighted network whose removal from the network resulted in the greatest increase in shortest distance between two specified nodes [25]. From the street connectivity point of view, Taylor (1999a, 1999b) described the role and function of dense network models for application to network reliability ([26, [27])). Liu and Frangopol (2005) studied network connectivity with respect to bridges and the bridge network expressed by the time-dependent reliability of connectivity between the origin and the destination locations [28].

CHAPTER 3. STREET CONNECTIVITY FRAMEWORK

We consider a residential area served by an on-demand bus service providing residents with transportation from/to their home to/from a major transit terminal (pick-up/drop-off customers). Passengers are able to book their rides by means of an Internet/phone service. One or more on-demand bus-stop nodes is assigned for each link of the road network. The length between two on-demand nodes is within the desired walking capacity of the passengers, which is usually 5 min of walk (or approximately 1200 ft) to a transit stop [29]. The distance between two on-demand nodes has to be much less than 1200 ft, as DRT shuttles serve passengers as close as possible to/from their location. Assigning on-demand bus-stop nodes helps both the bus operators and the passengers in serving at designated points along the cross-street link when there are multiple requests made for service at that link. The on-demand bus-stop nodes are not placed at the intersections. This is because mid-block bus stops are preferred for design, as they minimize sight-distance problems for the pedestrians and help create less pedestrian congestion at the passenger waiting areas [30]. Demand could arise anywhere within the service area following some spatial/temporal distributions and is assumed to be assigned to the closest stop (see Fig. 2). Passengers might be required to do some walking, but the overall service time is reduced when there are multiple requests made for service at that link. The shuttle departs from the terminal at pre-set intervals. Immediately before the beginning of each round trip, customers are scheduled by some algorithm and the route is constructed.

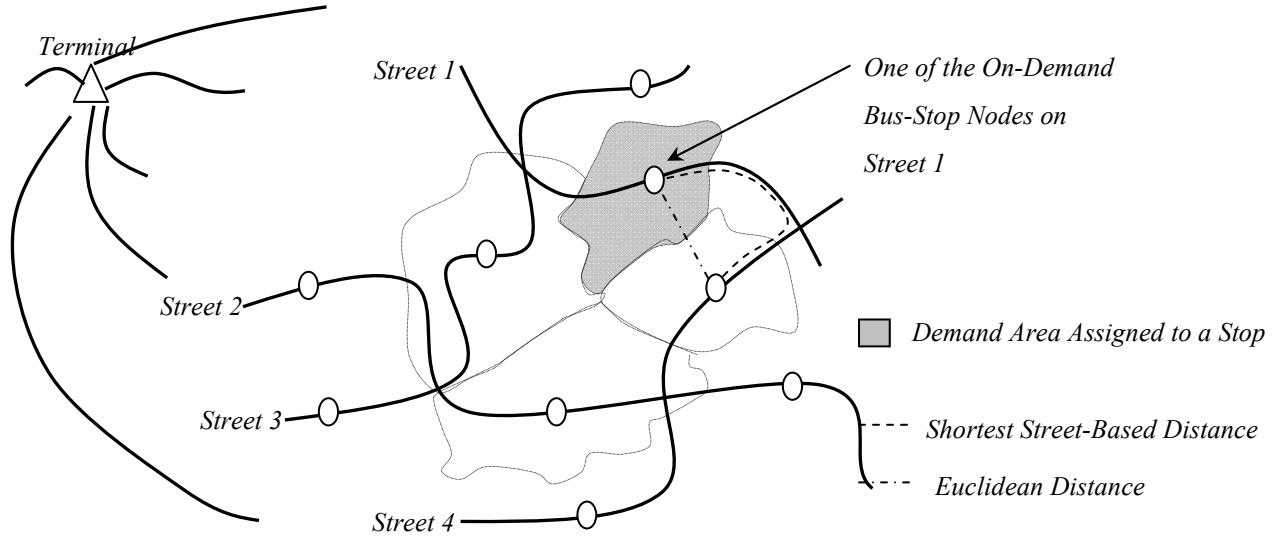


FIGURE 2: On-demand bus-stop nodes on cross-street links.

3.1 CONNECTIVITY INDICATOR

In this study, we revise and expand the definition of connectivity indicator found in Lam and Schuler (1982), which depends on a certain number of given travel times between demand points [31], as neither the street network geometry nor the passenger demand density is taken into account in computing the connectivity indicator.

The new connectivity indicator introduced in this research will be defined so that it can be a good predictor of the on-demand transit performance, which is usually composed by a weighed combination of operator's objective (lesser total distance traveled) and level of service (shorter waiting and in-vehicle riding times, assuming negligible walking time). Intuitively, all are dependent on how fast the shuttle is able to serve customers.

More rigorously, in a given service cycle, a set of n on-demand nodes (starting at the terminal $i = 0$ and returning back at the terminal $i = n + 1$) is scheduled for service by some

algorithm, and the total distance traveled is $D = \sum_{i=0}^n d_{i,i+1}$, where $d_{i,i+1}$ is the shortest path between any two consecutive stops i and $i + 1$. Thus, the expression for the cycle length or headway, C , can be represented as:

$$C = \left(\frac{D}{v} + nt \right), \quad (1)$$

where t is the average service time spent at each stop, and v is the average velocity of the shuttle.

If N is the total number of potential on-demand stops within the service area, $T = \sum_{i=1}^N \sum_{j=1}^N d_{ij}$ ($j \neq i$)

is the sum of all the shortest paths among all N nodes, and $T/[N(N-1)]$ is the average shortest path, it can be easily seen that D is a fraction f of T ($D = fT$).

For any general demand responsive transit system, the expected waiting time, $E(T_{wt})$, and expected in-vehicle riding time, $E(T_{rd})$, can be related to the headway using the following equations [19]:

$$E(T_{wt}) = (1 + \alpha) \frac{C}{2}, \quad (2)$$

where α is the proportion of passengers going from home to terminal (with $(1 - \alpha)$ as the proportion traveling from terminal to home), and

$$E(T_{rd}) = \frac{C}{2}. \quad (3)$$

Hence, using equations (1), (2), and (3):

$$E(T_{wt}) = \frac{(1 + \alpha)}{2} \left(\frac{fT}{v} + nt \right), \quad (4)$$

$$E(T_{rd}) = \frac{1}{2} \left(\frac{fT}{v} + nt \right). \quad (5)$$

Both are directly proportional to T . Hence, a desirable connectivity indicator of a given network should be proportional to T .

Since demand might be unevenly distributed among stops, some links are more likely to be used in a cycle and are therefore more critical than others for the overall transit performance. As an intuitive example, links connecting stops relatively far from the others but with little demand should not be considered as important as links connecting pairs of nodes with higher demand. Let λ_i be the demand per day or demand rate at i . We can assume that the likelihood for a pair of nodes i and j to be consecutive in a cycle (and the shortest path d_{ij} between them to be used) is proportional to the product of their demand rate λ_i and λ_j . We can therefore express the expected shortest path between any two nodes in a network as:

$$\sum_i \left[\frac{\lambda_i}{\sum_i \lambda_i} \left(\frac{\sum_j \lambda_j d_{ij}}{\sum_j \lambda_j} \right) \right], \quad \forall i, j \in \{1, 2, \dots, N\}, j \neq i, \quad (6)$$

which is equal to the average shortest path $T/[N(N-1)]$ (defined earlier) for demand equally distributed among nodes. Thus, a good CI taking into account demand spatial distribution should be related to (6).

3.2 PERFECT CONNECTIVITY FOR STREET NETWORKS

Most residential street patterns follow the grid form of street networks, as it is both pedestrian and vehicle friendly. Grid street patterns give plenty of route options for trips whether walking or using transit or private vehicle [32]. The maximum transit performance is reached, as this layout provides multiple route options.

An example of a grid street pattern is shown in Fig. 3 using the town of Hempstead, a residential town 50 mi northwest of downtown Houston, Texas, and there are several such grid networks all around the cities and towns of the U.S.



FIGURE 3: A grid section of the street network system of the town of Hempstead, TX (Source: Google Earth).

Consider a grid form of residential street pattern with each square-shaped unit of block size length s and spread infinitely across a very large area. Each potential passenger is located in a unit block area of s^2 , and the density of the demand is uniform as $\rho = (1/s^2)$. This assumption allocates every household demand a total of four potential bus stops for using the DRT service facility and, hence, would practically involve negligible passenger walking. We call this kind of street layout the perfect grid network system. This kind of street layout would naturally be preferred by the DRT passengers and also does away with setting up infrastructure for bus shelters. The desired connectivity needed for smooth DRT shuttle movement is also increased, as there are various route options to follow during trip scheduling.

The DRT scheduling trip is based on an algorithmic output for point-to-point service that is considered to be the closest to an optimal tour. Computing an optimal tour for the scheduled

pick-up/drop-off for the passengers is a traveling salesman problem (TSP)-like problem, which is considered to be *NP*-hard. Scheduling operations for DRT have always been a challenge for researchers. They involve TSP-like scheduling at several stages. Quadrifoglio and Dessouky (2004, 2007) and Quadrifoglio et al. (2006, 2007, 2008) approached DRT through the study of mobility allowance shuttle transit (MAST) service as the means of flexible transit systems ([33]-[37]). However, if we assume that the DRT shuttle picks a certain number of passengers during a given cycle length or the headway, the average closest distance between two random pick-up/drop-off passengers would be close to the optimal tour. Using this average closest distance between mutual pick-up/drop-off demands would also give a more accurate average lowest shuttle travel distance than that obtained using any available scheduling algorithm. Hence, in the next section, we derive this average closest distance between two random points over the perfect grid network system. The sketch in Fig. 4 below depicts a structural framework of an infinitely large grid network system.

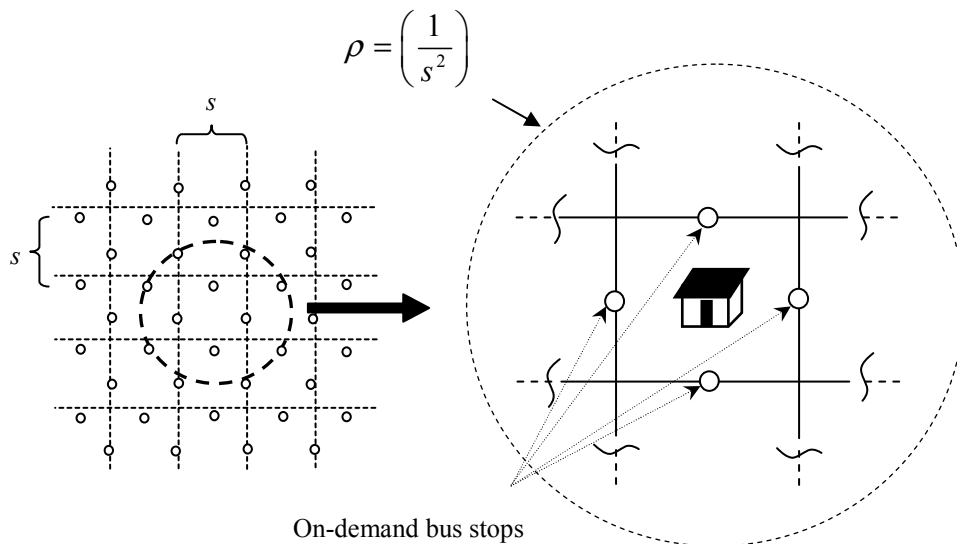


FIGURE 4: A perfect street network system.

3.2.1 AVERAGE CLOSEST STREET-BASED DISTANCE

We derive the expression for the average closest street-based distance between two uniformly distributed random demand points over an infinitely large perfect grid network. Consider an infinitely large street network system, as shown in Fig. 4 above. Uniformly and randomly scattered demand points follow a spatial Poisson distribution [38]. Assuming that the number of demand points Ω_A within the area A is a Poisson random variable, its distribution is given by:

$$P\{\Omega_A = x\} = \frac{(\rho A)^x}{x!} e^{-\rho A}, \quad (7)$$

where $x = 0, 1, 2, 3$, and so on.

For a zero demand to occur within the area A would imply $x = 0$, and the following expression is obtained:

$$P\{\Omega_A = 0\} = e^{-\rho A} \quad (8)$$

The passengers are expected to walk to the closest on-demand bus stop to avail the DRT service. This also means that the DRT shuttle would prefer to pick up the next closest passenger at the on-demand bus stop. Thus, using simple geometry, at present, if the DRT shuttle is at node Z , which could also be the terminal itself (see Fig. 5), the occurrence of a request for service within an assigned area A_n decides how far the n^{th} closest on-demand point is located on the grid street system. For example, the first closest demand point from Z will be located at a street-based distance of s if there is a request for service within the demand area of A_1 , as shown in Fig. 5. The second closest distance from the node Z is $2s$ when a request pops up in the next demand area of A_2 , and so on. The area is analyzed for a quarter section, as computation is easy.

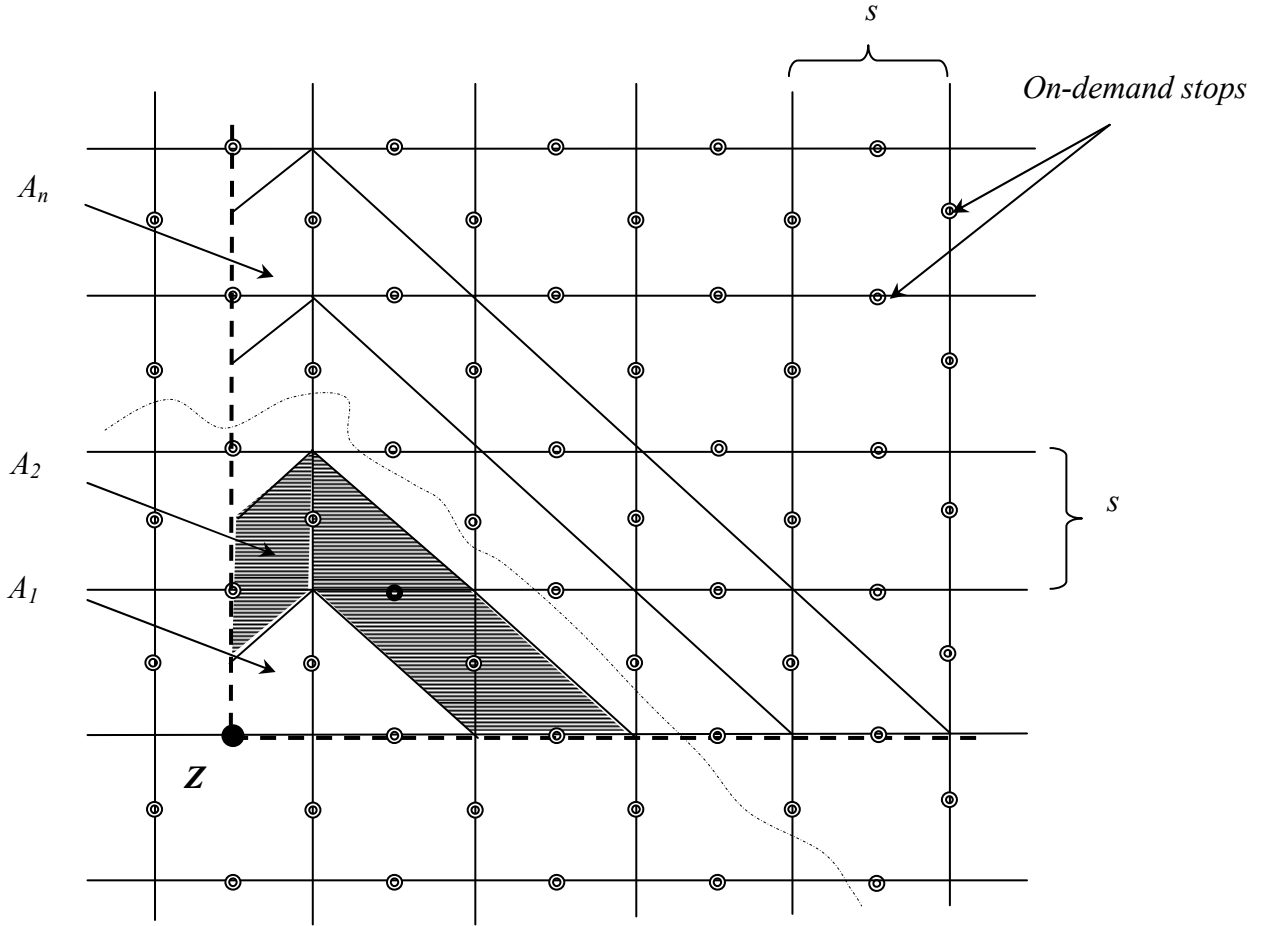


FIGURE 5: Locating the closest on-demand node from a known node Z.

Observing the geometry of each of the quarter sections in Fig. 5 above, the following expressions hold:

$$A_1 = \frac{s^2}{2} + \frac{3s^2}{8}; A_2 = \frac{(2s)^2}{2} + \frac{3s^2}{8} + \frac{s^2}{2}; \text{ or, in general, for the } n^{\text{th}} \text{ demand area,}$$

$$A_n = \frac{1}{2}(ns)^2 + \frac{3s^2}{8} + (n-1)\frac{s^2}{2} \quad (9)$$

Thus, the expected closest distance between two random demands $E[D]$ can be written as (using [8]):

$$\begin{aligned}
E[D] &= \sum_{n=1}^{\infty} (ns) P\{\Omega_A = 0\} = s \sum_{n=1}^{\infty} (n) e^{-4\rho A_n} = s \sum_{n=1}^{\infty} (n) e^{-2\rho s^2 \left(n^2 + (n-1) + \frac{3}{4} \right)} = s \sum_{n=1}^{\infty} (n) e^{-2\rho s^2 \left(n^2 + n - \frac{1}{4} \right)} \\
&= \left(s e^{\rho s^2} \right) \sum_{n=1}^{\infty} n e^{-2\rho s^2 \left(n + \frac{1}{2} \right)^2}
\end{aligned} \tag{10}$$

With $(\rho s^2 \geq 1)$, the variable n is small compared to the exponential terms with second power of n (where $n \geq 1$), and the expression for $E[D]$ is controlled primarily by the behavior of the exponential term. Hence, $E[D]$ can be written as:

$$E[D] \approx \left(s e^{\rho s^2} \right) \sum_{n=1}^{\infty} e^{-2\rho s^2 n^2} = \left(s e^{\rho s^2} \right) \sum_{n=1}^{\infty} \left(\frac{1}{e^{4\rho s^2}} \right)^{\frac{n^2}{2}} \tag{11}$$

Using the simplified expression for discrete normal distribution summation from [38] that satisfies the condition of $\left(\frac{1}{e^{4\rho s^2}} \right) \in (0, 1)$, the expression for $E[D]$ can be written as:

$$E[D] \approx \left(s e^{\rho s^2} \right) \sum_{n=1}^{\infty} \left(\frac{1}{e^{4\rho s^2}} \right)^{\frac{n^2}{2}} = \left(s e^{\rho s^2} \right) \left\{ \frac{1}{2} \left[\sqrt{\frac{\pi}{2\rho s^2}} \left(1 + 2 \sum_{n \geq 1} e^{-\frac{\pi^2 n^2}{2\rho s^2}} \right) - 1 \right] \right\} \tag{12}$$

Ignoring the summation terms, since $\left(2 \sum_{n \geq 1} e^{-\frac{\pi^2 n^2}{2\rho s^2}} \right) \ll 1$, $E[D]$ can be further simplified as:

$$E[D] \approx \left(\frac{s e^{\rho s^2}}{2} \left(\sqrt{\frac{\pi}{2\rho s^2}} - 1 \right) \right) \tag{13}$$

Further, we can simplify the expression in (13) using $\rho = \left(\frac{1}{s^2} \right)$ as:

$$E[D] \approx \left(\frac{s e}{2} \left(\sqrt{\frac{\pi}{2}} - 1 \right) \right) \approx 0.34s \tag{14}$$

Thus, a perfect street network connectivity is not only defined by an ideal grid street system (as shown in Fig. 5) with each house enclosed by four street links and having four on-demand bus stops but also with the DRT shuttle using the average closest distance to visit the next closest pick-up/drop-off passenger demand location. The expression in (14) can be fixed by assigning appropriate value of the block size length s depending on the maximum passenger walking distance to reach an on-demand bus stop. Thus, for a given value of s , the expression in (14) forms the value of the “perfect connectivity,” which takes into account the ideal street network configuration and a nearly optimal performance of the DRT shuttle for the most desirable service output.

Thus, in order to have the proposed CI directly (not inversely) proportional to transit performance and to cause an ideal CI identifying a perfect connectivity to be equal to 1 (as most indicators are defined), we finally define it as follows:

$$\text{Connectivity Indicator} = \frac{0.34s}{\sum_i \left[\frac{\lambda_i}{\sum_i \lambda_i} \left(\frac{\sum_j \lambda_j d_{ij}}{\sum_j \lambda_j} \right) \right]}, \quad (15)$$

where $d_{ij} = d_{ji} \forall i, j \in \{1, 2, \dots, N\}, j \neq i$.

This definition ensures that perfectly connected networks having ideal perfect connectivity would have a $CI = 1$. Any real network with the shortest paths calculated over the actual available links would have $CI \leq 1$.

The proposed CI is very easy to calculate for any street network system and should be a very good predictor of the on-demand transit performance; intuitively, the higher CI, the better the transit performance.

CHAPTER 4. STREET NETWORK MODELING

A uniform grid street network system with a square-shaped block size is selected for this research. This street network is ideal to analyze, as several other forms of street networks, such as rectangular, cul-de-sacs, etc., can be constructed by eliminating or adding new links to this uniform grid street network system. Each of the links is identified using different sets of on-demand nodes $N_{(x,y)}$, as is shown for one of the horizontal links in Fig. 6 (using solid circles in the “old” network while using empty circles to mark other links as nodes). These nodes are such that they represent the pick-up/drop-off points for the passengers in a random demand distribution setting. Mid-block stop locations also help in unnecessary interference with the upstream intersection [39]. Thus, the assigned vehicle in its course of its tour might or might not visit an on-demand node as decided by an appropriate scheduling procedure. This approach helps both the shuttle in not having to stop at too close a distance between two random pick-up/drop-off points as well as giving a designated stop for passengers. Hence, the block size s is such that it is within the desired walking capacity of the passengers to a transit stop [29]. The “new” network is formed by eliminating one of the horizontal links designated as $N_{(x,y)}$ of the old network. The notation $N_{(x,y)}$ is such that it is located at a horizontal distance of $(X - 0.5)s$ and a vertical distance of $(Y - 0.5)s$ from the origin $(0,0)$, where s stands for the block length of the network. Thus, we say, $X \in \{1, 2, \dots, q = (L/s)\}$ and $Y \in \{1, 2, \dots, m = (W/s)\}$, where, L and W are the length and width of the networks.

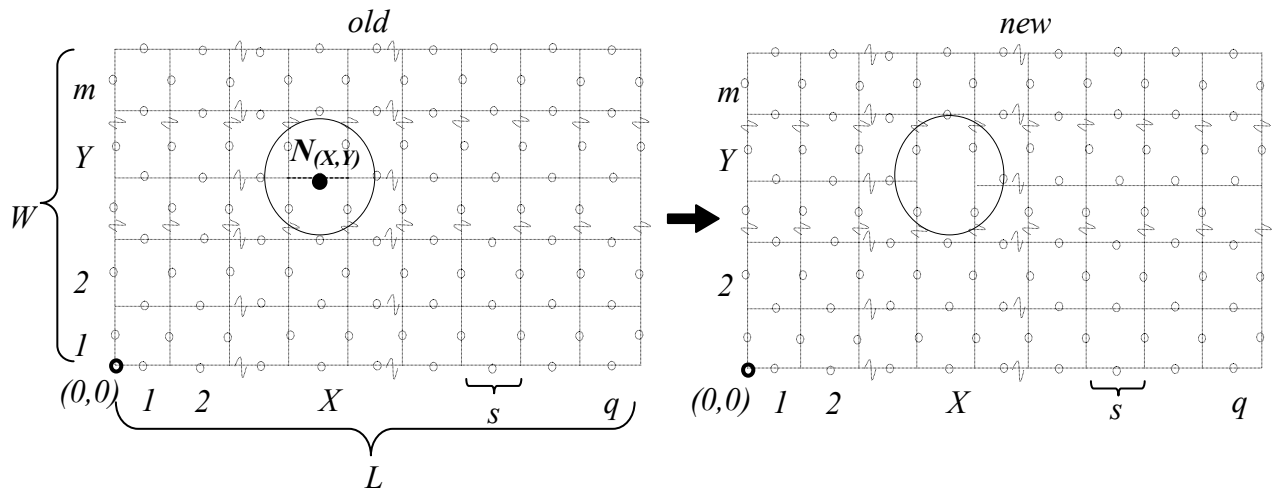


FIGURE 6: Removal of a link to create a new network from an old network.

The demand distribution is assumed to be uniform over the street network area. Thus, each on-demand node has equal probability of being selected for the service location. The choice of the grid network shown above falls in line with many of the existing real street networks within the urban and rural areas of the United States, such as that of Hempstead, Texas, as shown in Fig. 7. The choice of this network is also ideal, as there is a future proposal to build a commuter rail line connecting Hempstead to Houston, Texas [40].



FIGURE 7: Grid street system of Hempstead, TX (Source: Google Maps).

For a given DRT system, if a set of n on-demand nodes (starting at the terminal $i = 0$ and returning at the terminal $i = n + 1$) is scheduled for service by some algorithm, the total distance traveled is $D = \sum_{i=0}^n d_{i,i+1}$, where $d_{i,i+1}$ is the shortest path between any two consecutive stops i and $i + 1$. If N is total number of potential on-demand stops within the service area, $T = \sum_{i=1}^N \sum_{j=1}^N d_{ij}$ ($j \neq i$) is the sum of all the street-based shortest paths among all N nodes, and $T/[N(N - 1)]$ is the average shortest path, it can be easily seen that D is a fraction f of T ($D = fT$). Thus, the performance of the DRT shuttle is proportional to T , and the link that would have the largest change in the T due to its removal/closure would be counted as the most critical link in the network. We analyze the change in T using single link removal from the network and then generalize our findings for any given number of link removals. There are two ways in which a link can be removed under this case—a link placed horizontally can be removed or a link placed vertically can be removed. Now, consider that a node labeled as $N_{(x,y)}$ is removed from the network. The decrease in T consisting of all street-based shortest path distances from node $N_{(x,y)}$ (say $S_{(x,y)}$) to all other nodes in the network can be written as (see Appendix for derivation):

$$S_{(x,y)} = s \left(\begin{aligned} & (q+2)(m-Y+1)^2 + (m)(q-X+1)^2 + (3m+2) + \frac{(q-X)(q-X+1)}{2} \\ & + (q+2)(Y-1)^2 + (m)(X)^2 + \frac{(X-1)X}{2} - \left(\frac{Y(3Y-1)}{2} + \frac{(3m-3Y+5)}{2} (m-Y+2) \right) \end{aligned} \right) \quad (16)$$

The increase in T (say $R_{(x,y)}$) is:

$$R_{(x,y)} = 4(4qX - 4X^2 + 4X - 2q - 1)s \quad (17)$$

A detailed derivation for the expression for (16) and (17) is shown in the Appendix.

Thus, the net increase in T , (Δ_d), can be written as:

$$\Delta_d = R_{(X,Y)} - 2S_{(X,Y)} = \left\{ \begin{array}{l} 4(4qX - 4X^2 + 4X - 2q - 1)s \\ - \left(\begin{array}{l} 2(q+2)(m-Y+1)^2s + 2(m)(q-X+1)^2s + 2(3m+2)s \\ +(q-X)(q-X+1)s + 2(q+2)(Y-1)^2s + 2(m)(X)^2s + (X-1)Xs \\ -(Y(3Y-1)s + (3m-3Y+5)(m-Y+2)s) \end{array} \right) \end{array} \right\} \quad (18)$$

The multiplier term 2 in equation (18) is the back and forth distance, which is to be counted twice between the removed node and any other node.

For a given constant Y , the derivative of Δ_d with respect to X gives:

$$\begin{aligned} \frac{\partial \Delta_d}{\partial X} &= \left(\begin{array}{l} 16qs - 32Xs + 16s + 4(m)(q-X+1)s \\ +(q-X+1)s + (q-X)s - 4msX - Xs - (X-1)s \end{array} \right) \\ &= (18q + 4mq + 4m + 18 - 36X - 8mX)s \end{aligned} \quad (19)$$

$$\frac{\partial \Delta_d}{\partial X} = 0 \text{ when } X = \left(\frac{q+1}{2} \right) \text{ and}$$

$$\frac{\partial^2 \Delta_d}{\partial X^2} = -8m - 36 < 0.$$

Thus, for a given row (i.e., Y) Δ_d attains a maximum for $X = \left(\frac{q+1}{2} \right)$. The above result also holds for an odd q , since $X = \left(\frac{q+1}{2} \right)$ is a non-negative integer for any odd number q . For an even number q , we carry out the analysis in a slightly different manner. For a continuous discrete variable X , the expression for Δ_d is a discrete convex function and has a maximum at $X = \left(\frac{q+1}{2} \right)$. Thus, Δ_d would attain a maximum for an even q at $X = \left(\frac{q}{2} \right)$ or $X = \left(\frac{q}{2} + 1 \right)$, or both. We observe that for both $X = \left(\frac{q}{2} \right)$ and $X = \left(\frac{q}{2} + 1 \right)$, we obtain equal expressions of Δ_d as:

$$\begin{aligned}
\Delta_d &= \left(\begin{array}{l} 4(q^2 - 1)s - 2m\left(\frac{q}{2}\right)^2 s \\ -\left(\frac{q}{2}\right)^2 - \left(2m\left(\frac{q}{2}\right)^2 + 2mq + 2m\right)s - \left(\frac{q}{2}\right)^2 \end{array} \right) + f(Y) \\
&= \left(\frac{7(q)^2}{2} - mq^2 - 2mq - 2m - 4 \right) s + f(Y)
\end{aligned} \tag{20}$$

Further, if we fix X as constant and find the derivative of Δ_d with respect to Y for equation (20), Δ_d attains a maximum at $Y = \left(\frac{m}{2} + 1\right)$ and $Y = \left(\frac{m}{2}\right)$ for even m and at $Y = \left(\frac{m}{2} + 1\right)$ for odd m . This result follows from the symmetry of the street network structure along with the positions of the on-demand nodes. For example, the solid bars (not to scale) in Fig. 8 represent an approximate magnitude of the variation of Δ_d from $\Delta_{d,\max}$ to $\Delta_{d,\min}$ for individual link closure along the cross-section of the network for an odd q and odd m .

For a given row in the network system of Fig. 1 (i.e., given Y), Δ_d attains a maximum for $X = \left(\frac{q+1}{2}\right)$ and for an odd q . For an even number q , Δ_d would attain a maximum both for $X = \left(\frac{q}{2}\right)$ and $X = \left(\frac{q}{2} + 1\right)$. Further, if we fix X as constant, Δ_d attains a maximum at $Y = \left(\frac{m}{2} + 1\right)$ and $Y = \left(\frac{m}{2}\right)$ for even m and at $Y = \left(\frac{m+1}{2}\right)$ for odd m . This result also follows from the symmetry of the street network structure. As an illustration, the solid bars (not to scale) in Fig. 8 represent an approximate magnitude of the variation of Δ_d from $\Delta_{d,\max}$ to $\Delta_{d,\min}$ for individual link closure along the cross-section of the network for an odd q and odd m .

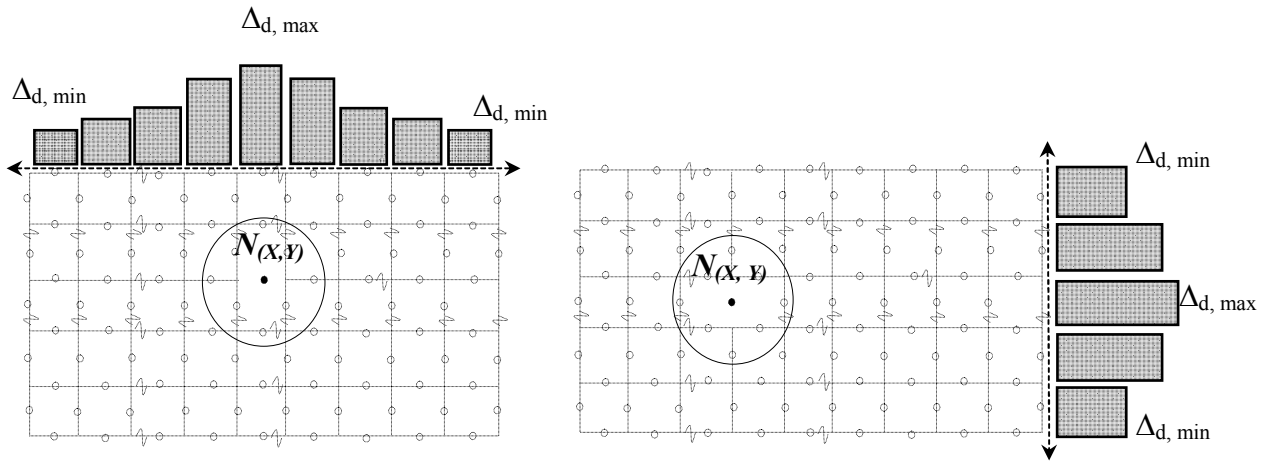


FIGURE 8: Variation of Δ_d along the cross-section of the street network.

Also, in situations when two or more combinations of links are simultaneously eliminated from the old network of Fig. 6, the resulting reduction in vehicular performance will be maximum when most of the central links are removed. However, we leave this discussion as our future research area.

CHAPTER 5. SIMULATION EXPERIMENTS

5.1 TESTING NEW CONNECTIVITY INDICATOR

The aim of the simulation is to demonstrate the robustness and the applicability of the proposed connectivity indicator (in equation (20)) for some reasonably assumed data sets and parameters. Different sets of connectivity indicator values are obtained for different street system configurations, and the DRT disutility values are noted. This is performed using programming in MATLAB R2010b. The street networks from different parts of Palm City, Florida, and Hempstead, Texas, as shown in Fig. 3, are used as an example for simulation. The demand density is assumed to be $\eta = 200$ passengers/day (in a 10-hr operation period), which the system can supposedly easily handle, as shown in the work of Chandra et al. (2011) with a similar service-area size. Other parameters considered in the simulation are outlined in Table 1.

Table 1: Simulation Inputs for Connectivity Indicator

Parameter	Input Numerical Values*
L^*	2050 ft
W^*	1750 ft
s^*	350 ft
V	20 mi per hour (i.e., the average speed in a residential area)
<i>Fleet size</i>	1
<i>Shuttle capacity</i>	infinite (or sufficient) to accommodate all passengers within a given cycle
<i>Dwell time</i>	30 sec (at the depot as well as at the pick-up/drop-off location)
<i>Headway**</i>	minimum of 8 min and maximum of 30 min at an interval of 1 min

*These are approximate values obtained using Google Earth. All street networks used are enclosed within this rectangular dimension.

**The minimum and maximum is such that optimal (or minimum) disutility is obtained within the range of headways used.

A very general disutility function (U) can be defined as:

$$U (\text{hr/passenger}) = q_1 w_t + q_2 w_r + q_3 w_k \quad (21)$$

where q_1 , q_2 , and q_3 are the weights for each of the performance components. These weights are difficult to determine; however, the more widely used and recommended values of $q_1 = 1.8$ and $q_2 = 1$ are used [41]. The contribution to disutility function due to average walking time of the passengers is not taken into account. This is mainly because DRT systems are designed to ensure negligible walking time of the passenger to a known stop. Thus, $q_3 = 0$. Other external factors, such as the bus-stop facility, shuttle comforts, etc., are not taken into account in computing the disutility function. As we are modeling a DRT system, the in-vehicle travel time or waiting time for the shuttle is small; thus, it would be reasonable to ignore factors accounting for the bus-stop or shuttle facility.

5.1.1 SIMULATION INPUT—PASSENGER REQUEST TIMES

The general work-trip data are obtained from the Bureau of Transportation Statistics webpage (BTS [2009]) for U.S. commuters, and they are primarily used as an input for generating passengers' random request times in the simulation [42]. The curves in Fig. 8 show the simplified form of the work-trip data as cumulative distribution functions (CDFs). The chart in Fig. 9 consists of two CDFs—the actual and the assumed density. The actual CDF (a polynomial of higher degree and, hence, difficult to invert) is the compilation of the raw data obtained from the BTS. The assumed CDF corresponds to the simply linearly varying version of the actual CDF.

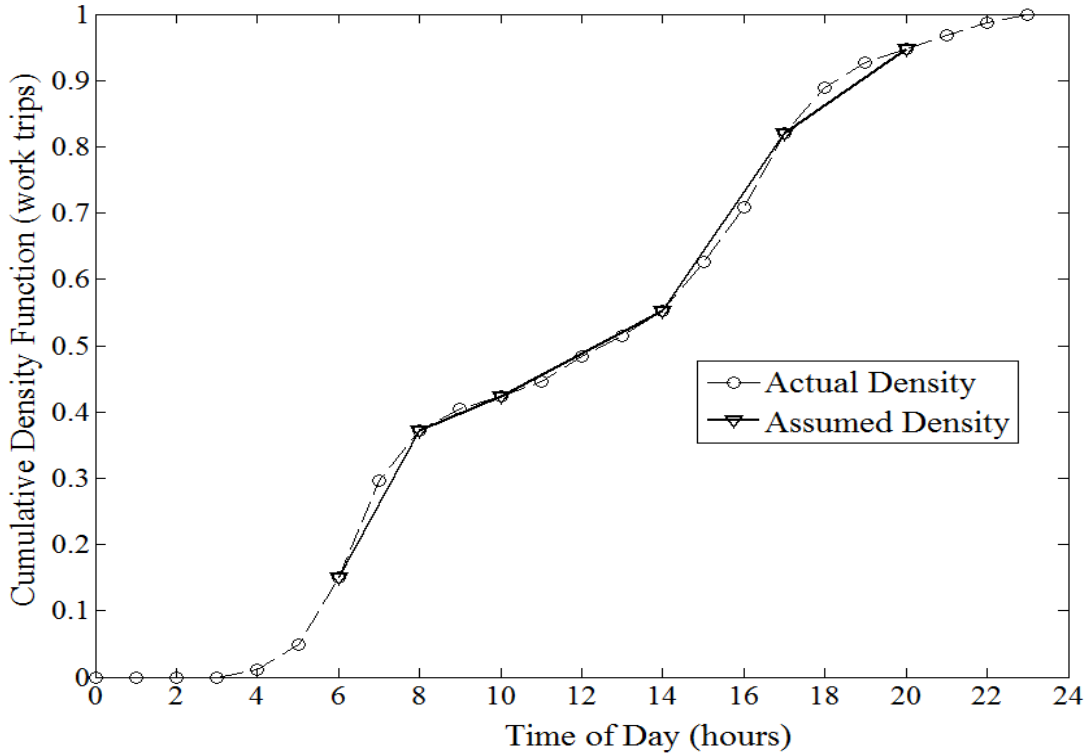


FIGURE 9: Cumulative density function for U.S. work trips for departure and arrival (arrival starts at 2 p.m.).

The piecewise linear CDF of the assumed density closely follows the actual existing distribution and is quite easy to invert for the random real number generated between 0 and 1. Each inverted random number (with respect to the linear assumed CDF) generates random request times of the passengers for a day. It is clearly observed (using either the actual or assumed CDF curves) that the majority of the departure times of commuters from their homes start around 6 a.m. and the arrival times to their homes start around 2 p.m. The service request times consist of either pick-up or drop-off requests by the passengers, and the prospective passengers book a reservation either on the Internet or by a phone call.

Some of the other inputs for the simulation model consist of:

- Distribution pattern of request time within each headway interval: uniformly random.

- Shuttle operational service timings: 6:30 a.m. to 11:30 a.m. (pick up) and 2:30 p.m. to 8:30 p.m. (drop off).
- Total service operation time: 10 hr.

The service shuttle is assigned for pick up/drop off starting from the terminal to the passenger demand nodes. The service requests are accepted either by phone or on the Internet between 6:00 a.m. and 8:00 p.m. The bus will stop at each node just once and in a manner to cover all the required nodes obtained using scheduling algorithms on its way back to the terminal. This is a TSP problem with the additional time constraint that the vehicle needs to be back at the terminal at the end of every given headway (or cycle length). The shortest street-based path between any two nodes is computed using Dijkstra's algorithm:

- Number of replications: 20.
- Trip scheduling algorithm: insertion heuristics.

Insertion heuristics evaluates and computes a sequence of the order of the requests for using the bus service for a given headway. The simulation model needs to define the bus headway beforehand to schedule the pick up or drop off. The output is the weighted sum of the expected waiting time and the expected in-vehicle riding time of the passengers, as represented before in the disutility evaluation using equation (21).

5.1.2 STREET NETWORK SYSTEM DESCRIPTION

A total of 10 different real street networks are used for this simulation exercise. Five of the first 10 street networks are the random subsets of the original connected streets of Fig. 3 of Hempstead. The assumption is that the transit agency could choose to serve just a selected number of streets within the original networks for DRT operations. The remaining five other streets are also some of the existing streets of different form and size from Palm City, Florida,

and the adjoining areas. These are shown in Fig. 10. As this study focuses only on the network connectivity, the choice of the location of terminal (shown using a solid box) is such that it does not greatly impact the transit performance. Thus, the terminals are placed as close as possible to the networks and yet are located on the middle of the leftmost periphery so that they can be treated as transfer points.

Each of the links of the real residential grid streets is represented using virtual solid dots that denote on-demand bus-stop nodes (as shown in Fig. 10). Node-to-node distance for all the networks used is approximately fixed at $s = 350$ ft, which is also the value for the block length of the grids of the streets from Hempstead, as was found using the Google Earth application. Maintaining equal node-to-node distance ensures that the passengers have a uniform choice of selecting a node for a pick-up/drop-off point once they walk onto the closest street. Though this node-to-node distance was fixed for the five street patterns from Hempstead, the distribution and location of nodes on the remaining five forms of streets are approximate. We selected this extent and size of networks for simulation, as it would have been computationally expensive to study DRT performance for an extremely large network.

Each of the sets of street systems shown in Fig. 10 is bounded by a dotted rectangle of a fixed L and W of values from Table 1 to accommodate demands from the residential houses located within a fixed boundary. Depending on the connectivity information of different networks within a fixed area, the transit operators can choose the best network for DRT operation. The passenger demands are assigned to the rectilinearly closest on-demand node. If we assume that the demand density is uniform over a given area, the demand that each node gets is proportional to the area that is closer to it than the other nodes. Thus, each node will have a different demand for the same uniform demand density over the street systems of Fig. 6.

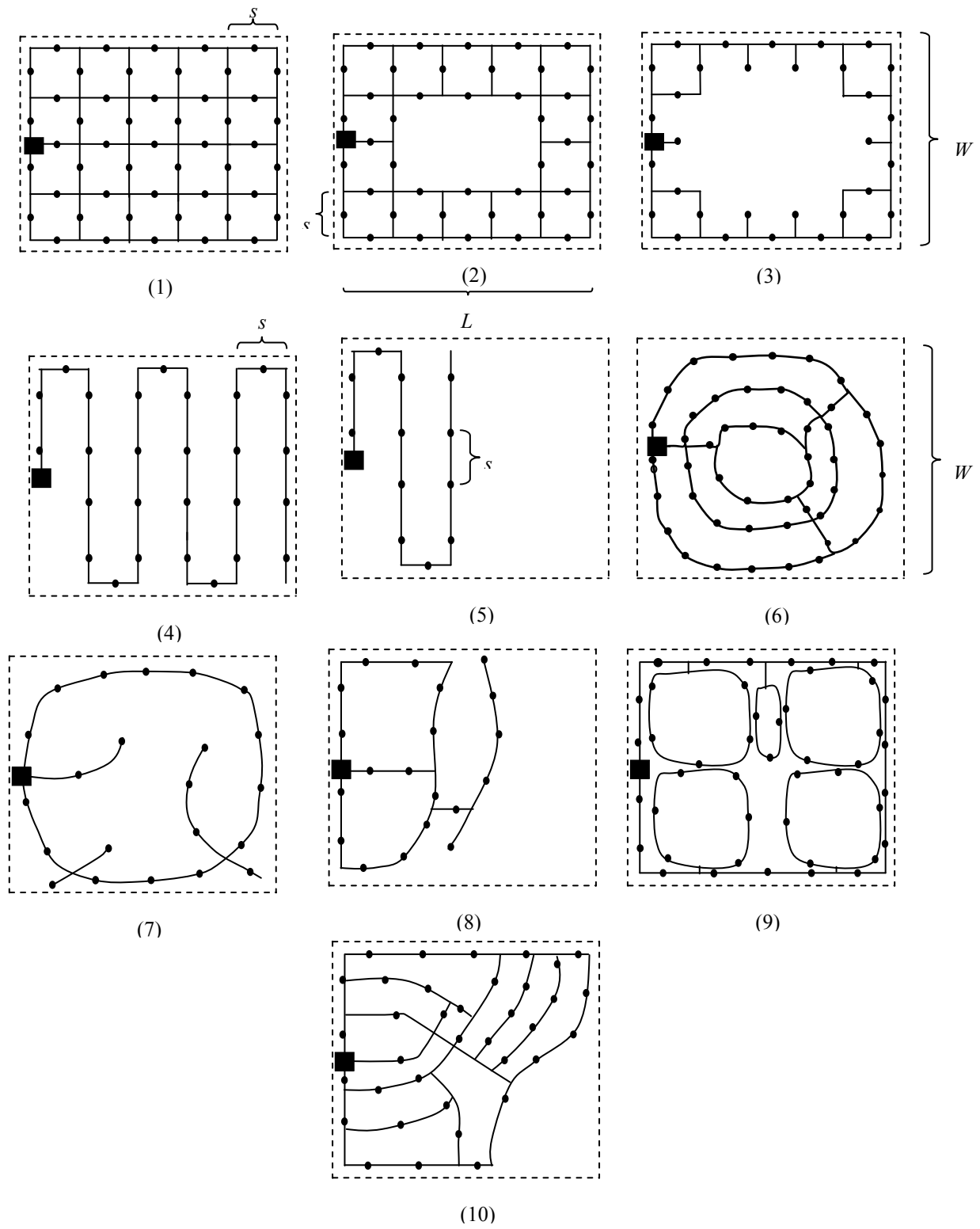


FIGURE 10: Examples of existing street patterns.

The four forms of street networks (2) and (3), though created from the residential streets (1) of Hempstead, represent street systems that are very likely to exist in reality. These street networks are usually seen in areas where there is a presence of a hill or a water body (such as a lake) around the central region of the network system. Sometimes the forest cover or the lake is created by the developers to maintain the aesthetic value or for increased livability conditions in a residential area. The elongated street systems like those of (4) and (5) can be seen in plenty of areas like Palm City, Florida [32]. The node-to-node distance among all networks of Fig. 10 is approximately 350 ft to maintain a uniformity of choice for passengers to choose their pick-up/drop-off node once they are on a street.

5.1.3 NUMERICAL CALCULATIONS OF CONNECTIVITY INDICES/INDICATORS

The new connectivity index values for networks (1) to (5) are calculated using the expression in equation (15). Planners can vary the value of s depending on the residential floor size standards needed for different residential towns and cities. We use an approximate value of $s = 400\text{ ft}$ based on a minimum block length requirement that forms within a walkable distance [5]. Besides the proposed one, the numerical values of two other widely acknowledged forms of indicators of connectivity—the first used in transportation planning and the second used in graph theory (Kansky, 1963), known as the Gamma index—are also computed for the five networks. The values are shown in Table 2. For a common scale comparison of performance/disutility variations among the three different connectivity indicators/indices, the revised connectivity values are used for the planning and the Gamma index (illustrated through plots in the later sections). The connectivity values (obtained in their revised forms) are scaled with respect to the new CI value of equation (15) obtained for network (5).

Table 2: Connectivity Index/Indicator Evaluated for the Five Networks

Network Number	<i>Connectivity Indicators</i>				
	Proposed Connectivity Index	Transportation Planning Connectivity Index		Gamma Index	
	Calculated	Calculated	Revised/Scaled	Calculated	Revised/Scaled
1	0.1069	0.3932	0.0456	1.1500	0.4363
2	0.1013	0.3465	0.0402	1.0128	0.3842
3	0.0724	0.3203	0.0371	0.9245	0.3507
4	0.0413	1.0000	0.1159	0.3209	0.1217
5	0.1160	1.0000	0.1159	0.3055	0.1159
6	0.0832	0.3392	0.0393	0.9831	0.3730
7	0.0922	1.0000	0.1159	0.3333	0.1265
8	0.1047	1.0370	0.1202	0.3457	0.1311
9	0.0622	1.1228	0.1301	0.4961	0.1882
10	0.1035	1.1552	0.1339	0.3851	0.1461

The graph theory measure of connectivity for planar graphs, known as the Gamma index, is expressed as $\left(\frac{e}{3(v-1)}\right)$, where v is the number of vertices present in the network and e is the number of edges connecting the vertices. A vertex is formed due to an intersection of two or more edges in the network. The end point of a free edge, such as that of a cul-de-sac or a dead end, is automatically counted as a vertex. This is the procedure used in calculating the Gamma index, as shown in Table 2. Thus, going by the definition of Gamma index, the higher the Gamma index, the greater connected the network, and vice-versa. As discussed earlier, the connectivity index in transportation planning is measured as the ratio of the total number of links to the total number of intersections in the network (for further reading, refer to Street Connectivity—Zoning and Subdivision Model Ordinance (2009), [43]). For this connectivity

measure used in planning, the higher the connectivity index value, the greater the connectivity of the network.

5.1.4 CONNECTIVITY INDICATOR—SIMULATION RESULTS AND DISCUSSIONS

The disutility values (U) are computed by simulating a DRT shuttle service for the networks of Fig. 10. It is observed (though not presented in this study) that in all the plots of the disutility value output obtained using simulation for varying headways, a typical convex curve is obtained with a well-defined minimum disutility for a unique headway. Thus, only the optimal (minimum) disutility values are reported, as it is expected that the transit agencies would prefer to achieve this minimum disutility during the operations of the DRT shuttle. The final simulation output is shown in Table 3 for different daily passenger demands of $\eta = 200$.

Table 3: Disutility Output Values for Different Networks

Network Number	Disutility (U)	Standard Deviation
1	0.570	0.053
2	0.580	0.054
3	0.638	0.085
4	0.925	0.057
5	0.546	0.033
6	0.633	0.049
7	0.587	0.064
8	0.575	0.039
9	0.775	0.050
10	0.580	0.049

Fig. 11 shows how each of the connectivity indicator values (from Table 2) compares with the optimal/minimum disutility values for a daily passenger demand of $\eta = 200$. The revised/scaled connectivity values (from Table 2) are used both for the transportation planning and the Gamma index, as shown below. The numbers on the Gamma index curve denote the network number.

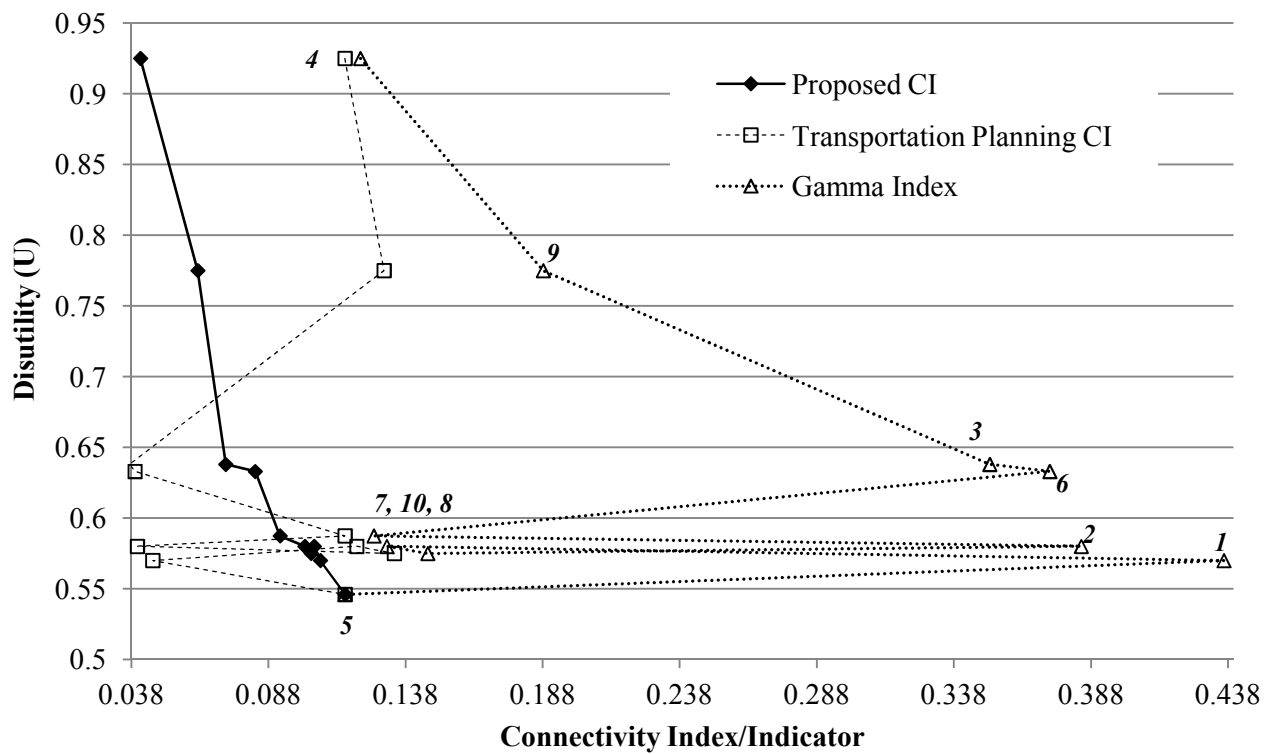


FIGURE 11: Variation of U versus different connectivity indicator values.

It is quite likely that the better or higher the connectivity is, the easier the vehicles will be able to navigate through the street networks, resulting in an increased ability of vehicles to reach their destination on time. However, it can be deduced from Fig. 11 that as the connectivity index from transportation planning and the Gamma index increase along the horizontal x-axis, the

disutility does not show a predictable or an intuitive variation. The Gamma index does better than the planning connectivity index in validating a general increasing trend in disutility for networks (6), (3), (9), and (4) as the connectivity decreases. However, the relationship between the performance of other networks and their Gamma index is extremely erratic. This clearly shows that performance cannot be very well related if the measure of connectivity from the graph theory concepts or from the transportation planners is used.

On the other hand, Fig. 11 shows that our proposed connectivity indicator does pretty well in expressing the decrease in disutility with a monotonic increase in the networks' connectivity. Thus, as per the definition of disutility, an increase in the values of our proposed connectivity indicator results in a decrease in the weighted sum of the expected waiting time and the expected riding times of the passengers. This predictable information would be quite useful for the transit agencies to assess a transit system's performance for a given network before it is even set up or put into operation.

Network (6) is further analyzed for performance with four different sets of demand distributions. These demand distributions are distributed differently for the on-demand nodes depending on their location. The image in Fig. 12 shows four different street systems, identified as (A), (B), (C), and (D), that connect their respective on-demand nodes.

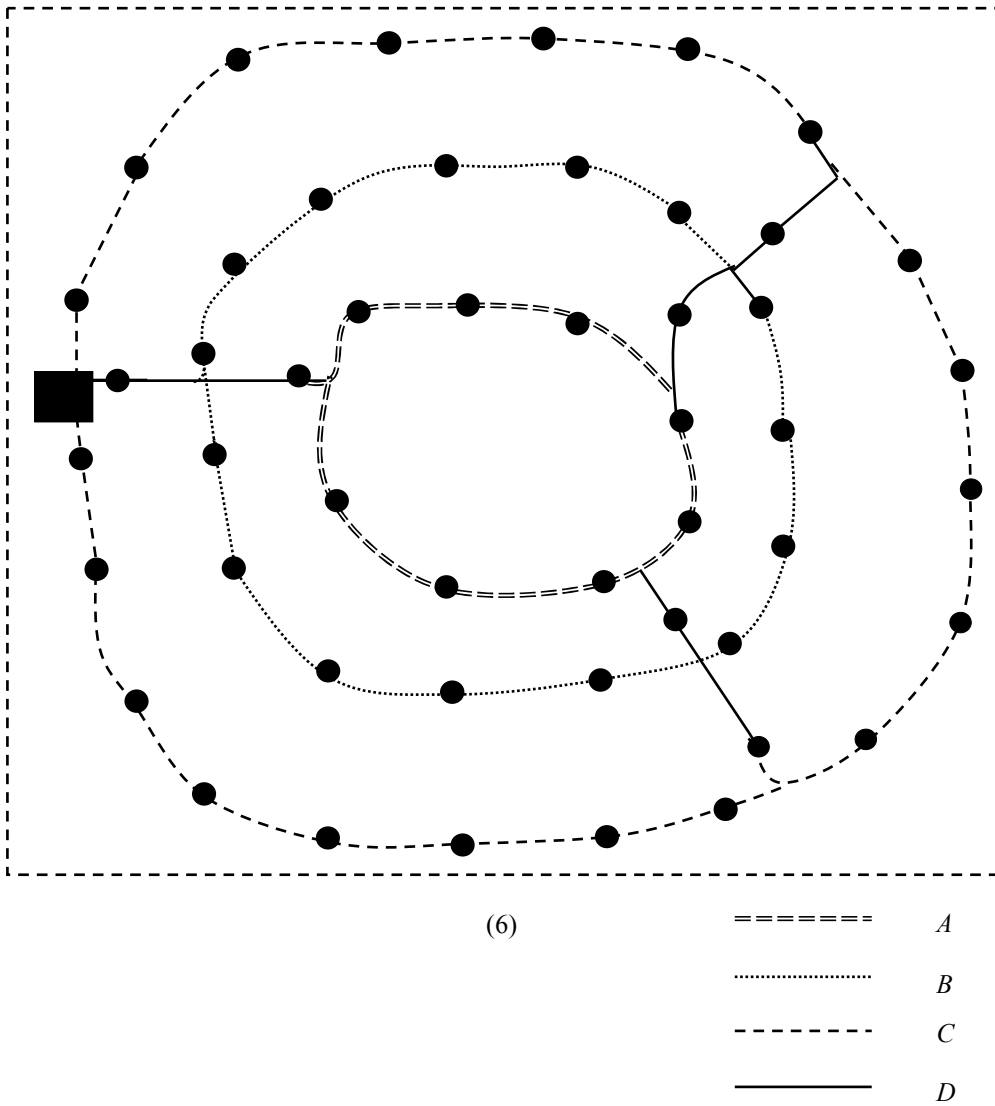


FIGURE 12: Different street systems within network (6).

The demand distribution varies with having the majority of the demands on one of the street systems to fewer demands on the rest in a sequential manner. Thus, while one street system has a very high demand, fewer demands exist at the other three street systems. These are identified as four different cases, from 1 to 4, where case 1 corresponds to a very high demand concentrated at the on-demand nodes of street system A, case 2 for street system B, and so on.

The simulation results for these cases are represented in Fig. 13 for different daily passenger demands of $\eta = 200$.

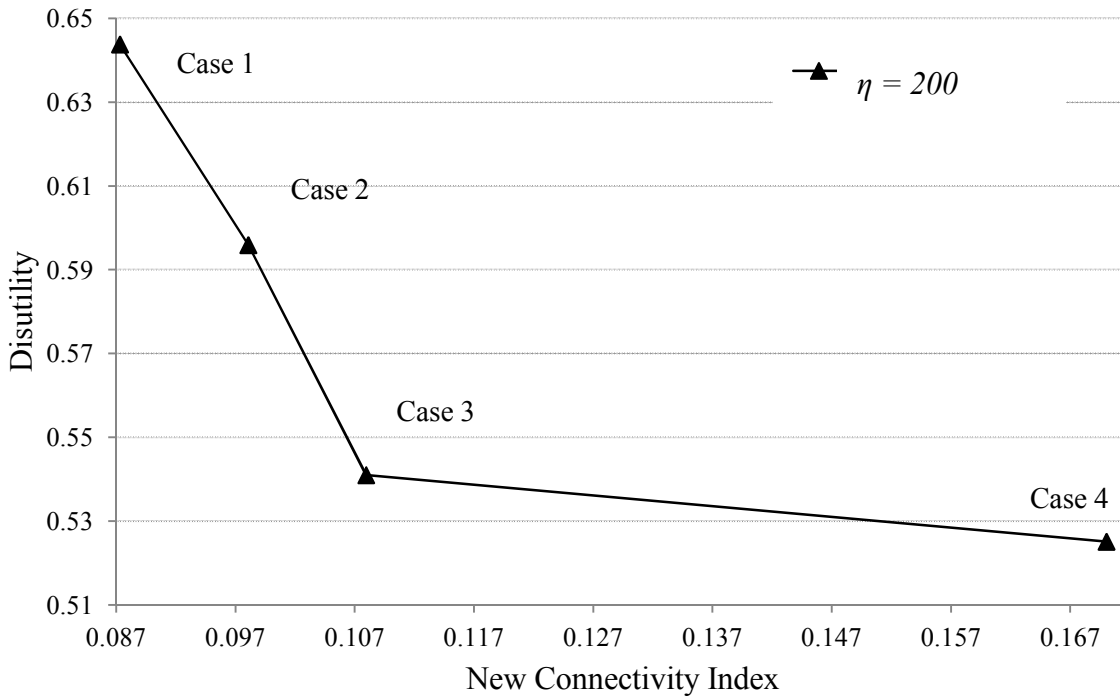


FIGURE 13: Disutility versus connectivity index variation for different demand distributions.

It is observed that different demand distributions within a given network of (6) cause a change in the connectivity indicator values. An increase caused in the proposed connectivity indicator by changing the spatial demand distribution does not change the trend of the fall in disutility. This further validates the versatility and applicability of the proposed connectivity indicator for DRT planning and designing over a given street network system.

5.2 SIMULATION TESTING FOR CRITICAL LINKS

We present some simulation results that validate the determination of critical links as shown above. A finite-size grid street network with identical blocks to the old network of Fig. 6 is selected, with some random links being removed in a sequence (1-2-3-4-5) each time (see Fig. 14). Hence, five different networks (in each a link missing) are used in the simulation.

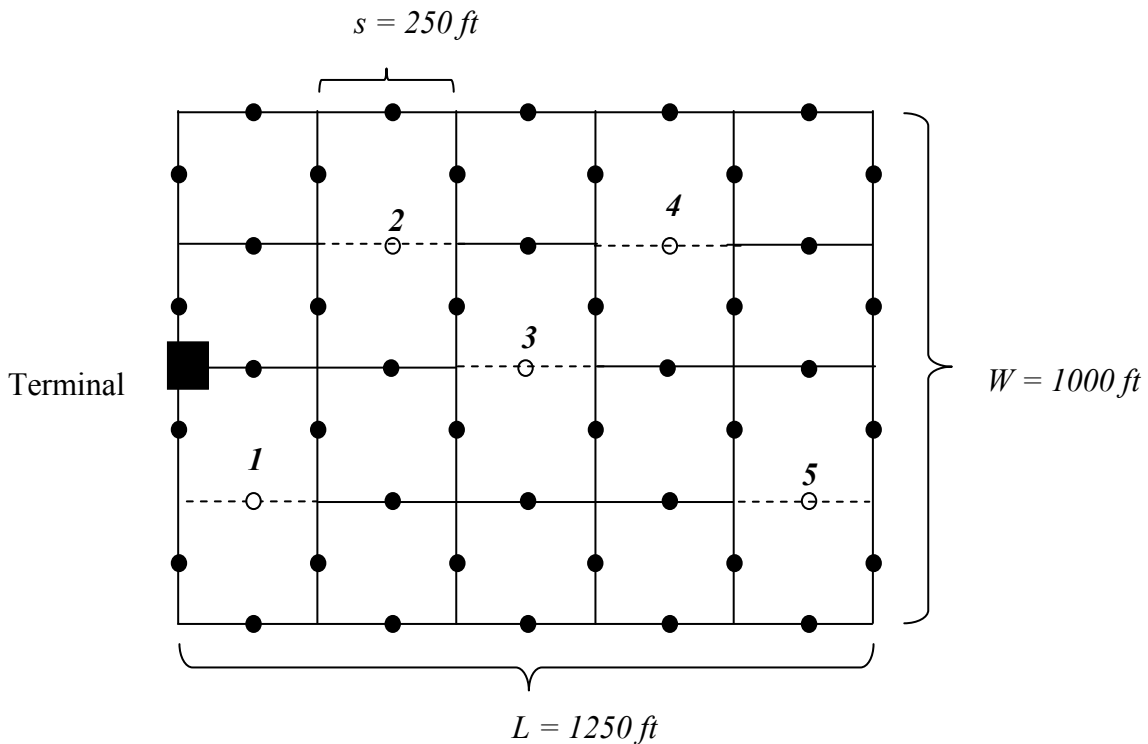


FIGURE 14: Sequential link closures/removals 1-2-3-4-5 to create five different sets of street networks.

A hypothetical DRT service that runs for a variable headway of 7.5 min to 21.5 min (assumed), serving a daily passenger demand of 300 (assumed) within a rectangular area of $L = 1250\text{ ft}$, $W = 1000\text{ ft}$, and $s = 250\text{ ft}$ (block size for Hempstead street network) is put in operation in all the five different grid networks (see Fig. 4). The DRT operational times are fixed from 6:30 a.m. to 9 p.m., and the passengers make random service requests generated from

typical travel demand hours of U.S. commuters, as shown in Fig. 8 earlier. Since the actual density (which is derived from real travel time data) is difficult to invert for generating passenger request times, the assumed density in its linearized form is used.

The requests for service usage are accepted between 6 a.m. through 8:30 p.m. by phone or Internet. These requests are randomly assigned as pick-up or drop-off requests. The spatially random service requests (within a given headway) are distributed uniformly over the on-demand nodes. These requests for service are either pick-up or drop-off with a fixed DRT terminal. The order of pick-up/drop-off of passengers, within each of the headways, is carried out using insertion heuristic [36]. The street-based shortest path distance between two nodes is computed using Dijkstra's algorithm coded in MATLAB R2010b [44].

The DRT performance can generally be identified as a combination of operating costs and service quality. The service quality is expressed as passengers' disutility: a weighted sum of expected waiting time and expected in-vehicle travel time (in the ratio of 1:1.8) typically used for any DRT service [41]. The performance values are obtained from an average of 10 numbers of replications for each of the five networks for different links removed and are shown in Fig. 15.

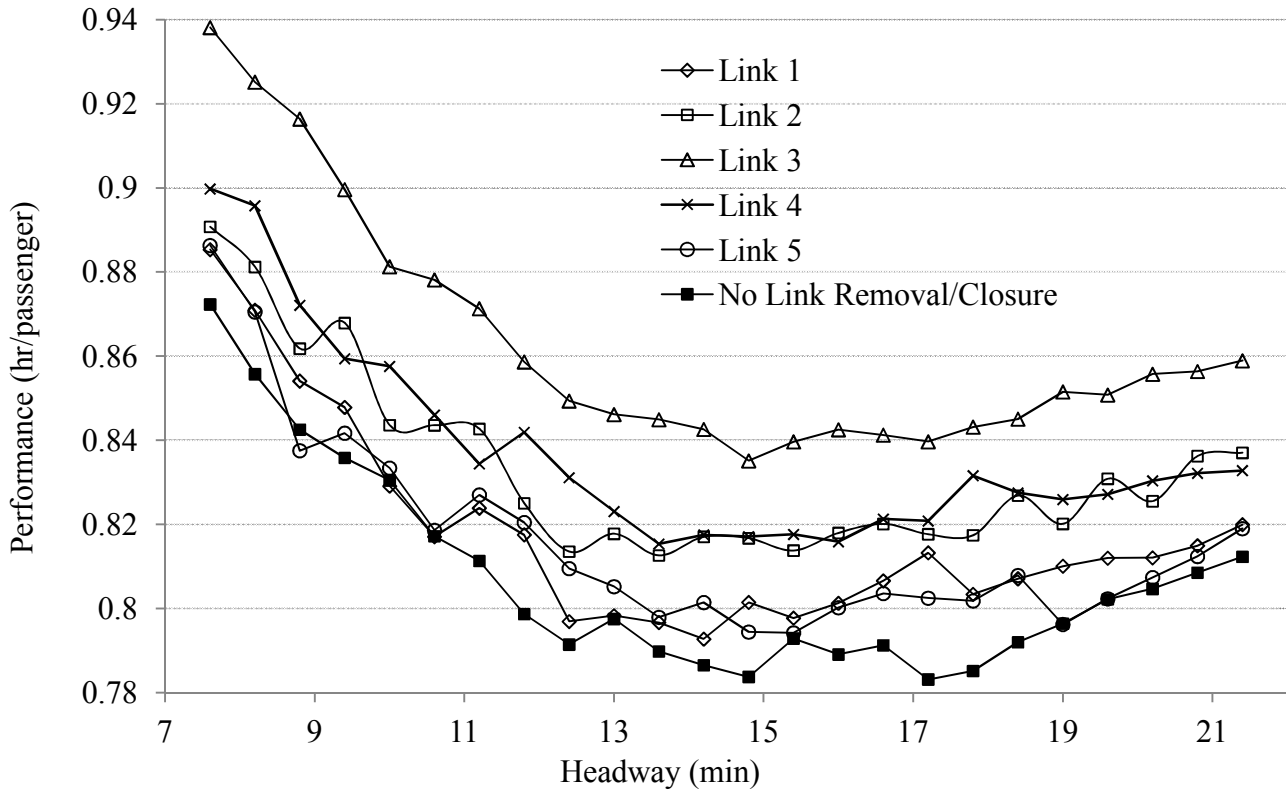


FIGURE 15: Performance effects on DRT for the sequential link closures/removals.

Fig. 15 shows that the removal of link 3 results in an increase in the average waiting and riding time of the passengers the most. Link 1 and link 2 case removal conditions show a very close resemblance in performance with link 4 and link 5 case removals, respectively, while for a “no link removal/closure” condition, the performance of the transit shuttle is the best. Thus, simulation results validate our analytical modeling of the critical link’s identification when q (or m) is odd.

CHAPTER 6. CONCLUSIONS

In this report, we provide general insights on the relationship between the street network system connectivity and the transit system performance, especially DRT. Two major connectivity measurement tools that have been developed in the past are discussed along with the drawbacks for each. An absence of a proper connectivity measuring technique for a simplified grid network system motivated us to propose a connectivity index definition that is easy to use and apply for a general grid system kind of street pattern with several cul-de-sacs. The most important contribution of this study is to fulfill the need for a better understanding of the role street connectivity plays in a transit system's performance, which has been aptly justified with the simulation results. As the steady outlawing of cul-de-sac street patterns continues in most cities of the U.S., the proposed connectivity definition can be quite handy for city planners and engineers in the future.

This study presents an analytical model to assess link criticality important for a desirable vehicular or transit shuttle performance. The contribution of this work is the closed-form equation that identifies the critical links for any grid network size and thus allows for the avoidance of exhaustive computations or approximations. It is found that for a grid street network system, the links located at the interior of the network are more critical than those located at the periphery, and this is validated through sets of simulation experiments. Though this work mainly focuses on studying a grid network system, a large form of other network structures, such as cul-de-sacs, rectangular patterns, etc., can be analyzed with a similar logic as that presented in this study. This will be the future research focus for the authors.

Future research will focus on analyzing other performance parameters such as the average waiting time and the average riding time that influence multimodal ridership. The

routing strategy of feeder buses in each of the service zones with street networks can be decided or assumed appropriately to derive analytical expressions for the performance. Further, simulations can be performed to validate the derivations.

REFERENCES

- [1] American Public Transportation Association, Accessed 28 Dec 2010,
http://www.apta.com/resources/statistics/Documents/Ridership/2010_q3_ridership_APTA.pdf
- [2] Dial-a-Ride Transportation (DART), <http://www.dialaride.org/index.htm> (Accessed 20 October 2009).
- [3] Southworth M, Owens PM. (1993). The evolving metropolis: studies of community, neighborhood, and street form at the urban edge. *J Am Plann Assoc.*, vol. 59, pp. 271-287.
- [4] Virginia Department of Transportation (VDOT),
http://www.vdot.virginia.gov/projects/resources/SSAR_Summary_03-20-09.pdf (Accessed 12 December 2010).
- [5] Handy, S., R.G. Paterson, and K. Butler. (2003). Planning for Street Connectivity: Getting from Here to There. *American Planning Association*, PAS Report Number 515.
- [6] Frank, L. D., B. Stone Jr. and W. Bachman. (2000). Linking land use with household vehicle emissions in the central Puget Sound: methodological framework and findings. *Transportation Research Part D*, vol. 5, pp. 173-196.
- [7] Cervero, R. and K. Kockelman. (1997). Travel Demand and the 3Ds: Density, Diversity, and Design. *Transportation Research D*, vol. 2, pp. 199-219.
- [8] Plan it Calgary—Local Transportation Connectivity Study, December 2008,
www.calgary.ca/planit/ (Accessed 22 August 2010).
- [9] Steiner, F and K. Butler. (2007). *Planning and Urban Design Standards*, John Wiley & Sons, Inc.

- [10] Peponis, J., D. Allen, D. Haynie, M. Scoppa and Z. Zhang. (2007). Measuring the Configuration of Street Networks. In the *6th International Space Syntax Symposium*, Istanbul, Turkey.
- [11] Peponis, J., S. Bafna and Z. Zhang. (2008). The Connectivity of Streets: Reach and Directional Distance. *Environment and Planning B: Planning and Design*, vol. 35 no 5, pp. 881-901.
- [12] Kansky, K.J. (1963). Structure of Transportation Networks: Relationships between Network Geometry and Regional Characteristics (University of Chicago, Chicago, 1963).
- [13] Derrible, S. and C. Kennedy. (2009). Network Analysis of World Subway Systems Using Updated Graph Theory. *Transportation Research Record: Journal of the Transportation Research Board*, vol. 3, pp.17-25.
- [14] Derrible, S. and C. Kennedy. (2010a). Characterizing Metro Networks: State, Form, and Structure. *Transportation*, vol. 37 (2), pp. 275-297.
- [15] Derrible, S. and C. Kennedy. (2010b). The Complexity and Robustness of Metro Networks. *Physica A: Statistical Mechanics and its Applications*, vol. 389, no. 17, pp. 3678-3691.
- [16] Gleason, J.M. and D.T. Barnum. (1986). Toward Valid Measures of Public Sector Productivity: Performance Measures in Urban Transit. *Management Science*, vol. 28 no. 4, pp. 379-386.
- [17] Fielding G.J., T.T. Babitsky and M.E. Brenner. (1985). Performance Evaluation for Bus Transit. *Transportation Research Part A: General*, vol. 19(1), pp. 73-82.
- [18] Badami, G. Madhav and H. Murtaza. (2007). An Analysis of Public Bus Transit Performance in Indian Cities. *Transportation Research Part A: Policy and Practice*, vol. 41(10), pp. 961-981.

- [19] Quadrifoglio L. and X. Li. (2009). A Methodology to Derive the Critical Demand Density for Designing and Operating Feeder Transit Services. *Transportation Research, Part B: Methodological*, vol. 43, pp. 922-935.
- [20] Chandra S., C. Shen and L. Quadrifoglio. (2011). A Simulation Study to Derive the Optimal Cycle Length for Feeder Transit Services. *International Journal of Information Systems in the Service Sector*, vol. 3(3), pp. 27-47.
- [21] Jenelius, E., T. Petersen, T. and L.-G. Mattsson. (2006). Importance and Exposure in Road Network Vulnerability Analysis. *Transportation Research Part A*, vol. 40, pp. 537-560.
- [22] Knoop, V.L., M. Snelder, and H.J. Van Zuylen. (2007). Comparison of Link-Level Robustness Indicators. In *Proceedings of the Third International Symposium on Transportation Network Reliability (INSTR07)*, ed. H.J. Van Zuylen, Paper no. 82. Delft, The Netherlands: Delft University of Technology.
- [23] Taylor, M. A. P., S. V. C. Sekhar, and G. M. D'Este. (2006). Application of Accessibility Based Methods for Vulnerability Analysis of Strategic Road Networks. *Networks and Spatial Economics*, vol. 6, pp. 267-291.
- [24] Ball, M.O. and B.L. Golden. (1989). Finding the Most Vital Arcs in a Network. *Operations Research Letters*, vol. 8, pp. 73-76.
- [25] Corley, H.W. and D.Y. Sha. (1982). Most Vital Links and Nodes in Weighted Networks. *Operations Research Letters*, vol.1, pp. 157-160.
- [26] Taylor M.A.P. (1999a). Dense Network Traffic Models, Travel Time Reliability and Traffic Management. I: General Introduction. *Journal of Advanced Transportation*, vol. 33(2), pp. 218-233.

- [27] Taylor M.A.P. (1999 b). Dense Network Traffic Models, Travel Time Reliability and Traffic Management. II: Application to Network Reliability. *Journal of Advanced Transportation*, vol. 33(2), pp. 235-251.
- [28] Liu M. and D. M. Frangopol. (2005). Balancing Connectivity of Deteriorating Bridge Networks and Long-Term Maintenance Cost through Optimization. *J. Bridge Engrg.*, vol.10(4), pp. 468-481.
- [29] S. O’Sullivan and J. Morrall. (1996). Walking Distances to and from Light-Rail Transit Stations. *Transportation Res Record*, vol. 1538, pp. 19-26.
- [30] Guidelines for the Location and Design of Bus Stops. (1996). *Transit Cooperative Research Program-19*, Texas Transportation Institute at Texas A&M University.
- [31] Lam, T.M. and H.J. Schuler. (1982). Connectivity Index for Systemwide Transit Route and Schedule Performance. *Transp. Res. Rec.*, vol. 854, pp. 17-23.
- [32] Kostof, S. (1991). *The City Shaped*. Boston: Little, Brown.
- [33] Quadrifoglio, L. and M. Dessouky. (2004). MAST Services: Formulation and Simulation Comparison with Conventional Fixed Route Bus Services. *4th IASTED International Conference on Modeling, Simulation and Optimization (MSO)*, Kauai, Hawaii, USA, August 2004.
- [34] Quadrifoglio, L. and M. Dessouky. (2007). Sensitivity Analyses over the Service Area for Mast Services. *Computer-Aided Systems in Public Transport*, M. Hickman, P. Mirchandani, and S. Voss (eds.), *Lecture Notes in Economics and Mathematical Systems*, 600, Springer (Heidelberg), pp. 419-432.
- [35] Quadrifoglio, L., R.W. Hall and M. Dessouky. (2006). Performance and Design of Mast Services: Bounds on the Maximum Longitudinal Velocity. *Transportation Science*, 40, 351-363.
- [36] Quadrifoglio, L., M. Dessouky and K. Palmer. (2007). An Insertion Heuristic for Scheduling Mast Services. *Journal of Scheduling*, vol. 10, pp. 25-40.

- [37] Quadrifoglio, L., M. Dessouky and F. Ordóñez. (2008). Mast Services: MIP Formulation and Strengthening with Logic Constraints. *European Journal of Operational Research*, vol. 185, pp. 481-494.
- [38] Szablowski P.J. (2001). Discrete Normal Distribution and its Relationship with Jacobi Theta Functions. *Statistics and Probability Letters*, vol. 52, pp. 289-299.
- [39] Guidelines for the Location and Design of Bus Stops, *Transit Cooperative Research Program-19*, Texas Transportation Institute at Texas A&M University (1996).
- [40] Community Impact Newspaper, <http://impactnews.com/northwest-houston/328-news/8428-city-plans-commuter-rail-tod> (Accessed 23 June 2011).
- [41] Wardman, M. (2004). Public Values of Time. *Transport Policy*, vol.11 (4), pp. 363-377.
- [42] Bureau of Transportation Statistics, (2009).
http://www.bts.gov/publications/national_transportation_statistics/2005/index.html (Accessed June 2010).
- [43] Street Connectivity—Zoning and Subdivision Model Ordinance. (2009). Division of Planning, Kentucky Transportation Cabinet.
- [44] Online Documentation, *MATLAB R2008b*,
<http://www.mathworks.com/access/helpdesk/help/helpdesk.html> (Accessed 6 January 2011).

APPENDIX

Let us define a “target” node to which we compute the sum of total distances from all on-demand nodes. This target node (shown as a solid circle; empty circles are on-demand nodes or just nodes) is located at the lower horizontal line of the bottom corner grid of the street network system, as shown in Fig. 16.

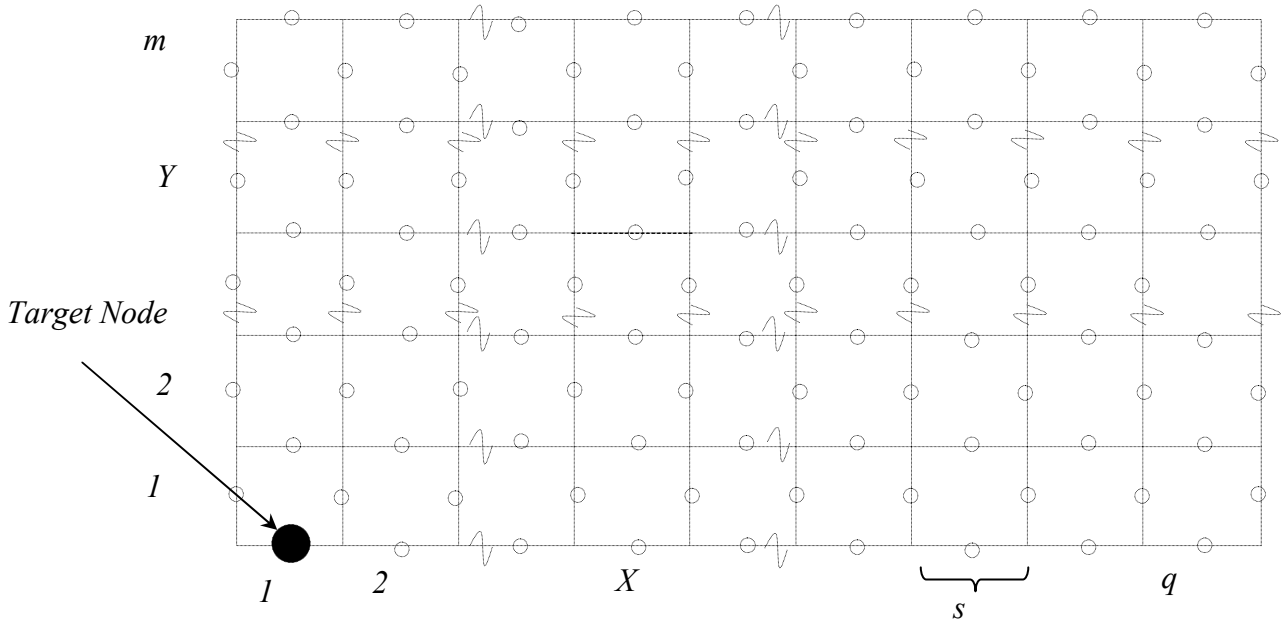


FIGURE 16: Sketch depicting the target node in the street network system.

In the above figure, we have a total of $(2m + 1)$ series of nodes that are distributed horizontally and $(2q + 1)$ series of nodes distributed vertically. Let $T_{(2m+1-2k)}$ denote the sum of distances from the target node to a series of unnumbered horizontal nodes just above a numbered horizontal series k ($k \in \{0, 1, 2, \dots, m\}$), with the last sum being $T_{(2m+1)}$ for $k = 0$. Also, let $T_{(2m+2-2p)}$ stand for the sum of distances to the target node from numbered horizontal nodes

$p \in \{1, 2, \dots, m\}$, with the last sum being $T_{(2m)}$ for $p = 1$. Thus, in terms of constant m , we have:

$$\begin{aligned}
 T_1 &= \left\langle \frac{q(q-1)s}{2} + s + qms \right\rangle \\
 T_2 &= \left\langle \frac{q^2s}{2} + \frac{s}{2} + (q+1)\left(ms - \frac{s}{2}\right) \right\rangle \\
 &: \\
 &: \\
 T_{2m} &= \left\langle \left(\frac{q^2s}{2} + \frac{s}{2} \right) + (q+1)\left(ms - \frac{(2m-1)s}{2} \right) \right\rangle, \text{ and} \\
 T_{2m+1} &= \left\langle \left(\frac{q(q-1)s}{2} + s \right) + q\left(ms - \frac{2ms}{2} \right) - s \right\rangle.
 \end{aligned}$$

Thus, summation of all the above terms in T_i with $i = \{1, 2, \dots, 2m + 1\}$ would give us the sum of all distances from all the nodes of the street network system to the target node. It can be easily computed using some rearrangement of terms as an arithmetic progression series:

$$\sum_{k=0}^m T_{2m+1-2k} + \sum_{p=1}^m T_{2m+2-2p} = \sum_{i=1}^{2m+1} T_i = \left\langle qm^2s + (m^2s/2) + mq^2s + \frac{3ms}{2} + \frac{q(q-1)s}{2} \right\rangle \quad (23)$$

Using the above result for the sum of the distances from all nodes of the network to the target node, we can derive an expression for any general on-demand node to all other on-demand nodes. First, we notice that we can treat any intermediate node in the network system as a ‘‘shifted target node’’ with the total area divided into four regions, such as A , B , C , and D , as shown in Fig. 17.

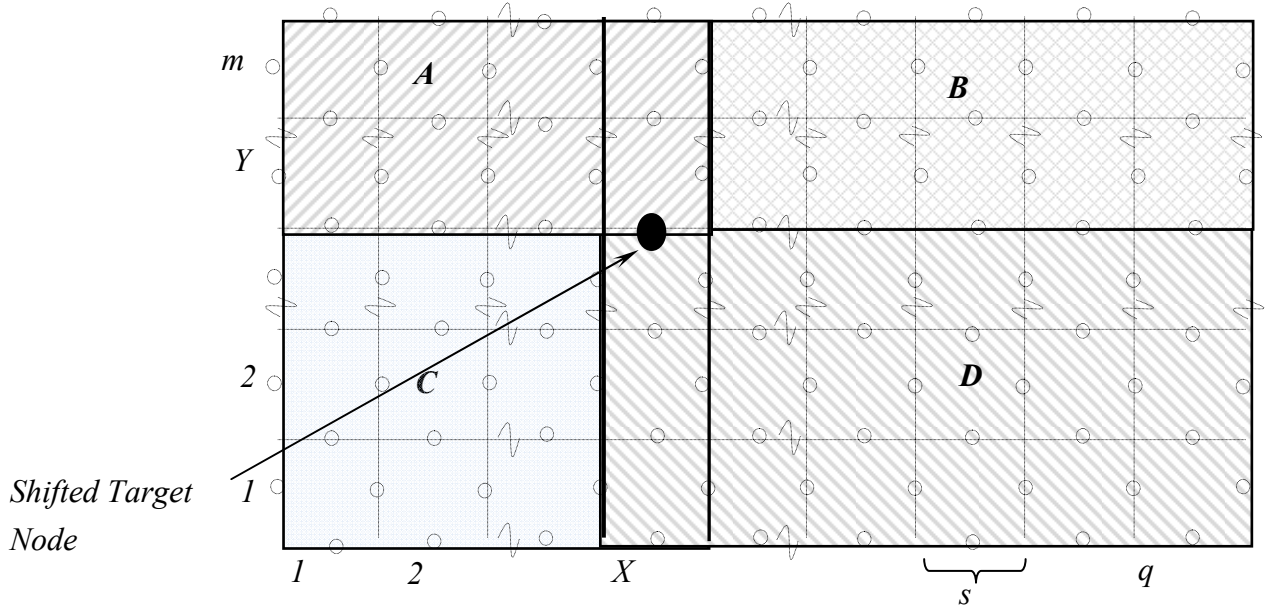


FIGURE 17: Split regions to create target node for any intermediate node.

The shifted target node lies such that there is an overlapping area of A, B, C, and D that needs to be accounted for (see Fig. 17 above). Thus, the sum of distances from all the nodes of each of the respective four regions (say $S_{(X,Y)}$) to this target node is derived and written in final form as:

$$S_{(X,Y)} = \left(\begin{aligned} & (q+2)(m-Y+1)^2 s + (m)(q-X+1)^2 s + (3m+2)s + \frac{(q-X)(q-X+1)s}{2} \\ & + (q+2)(Y-1)^2 s + (m)(X)^2 s + \frac{(X-1)Xs}{2} - \left(\frac{Y(3Y-1)}{2} s + \frac{(3m-3Y+5)}{2} (m-Y+2)s \right) \end{aligned} \right) \quad (24)$$

Then, the sketch in Fig. 18 is used to derive the expression for $R_{(X,Y)}$.

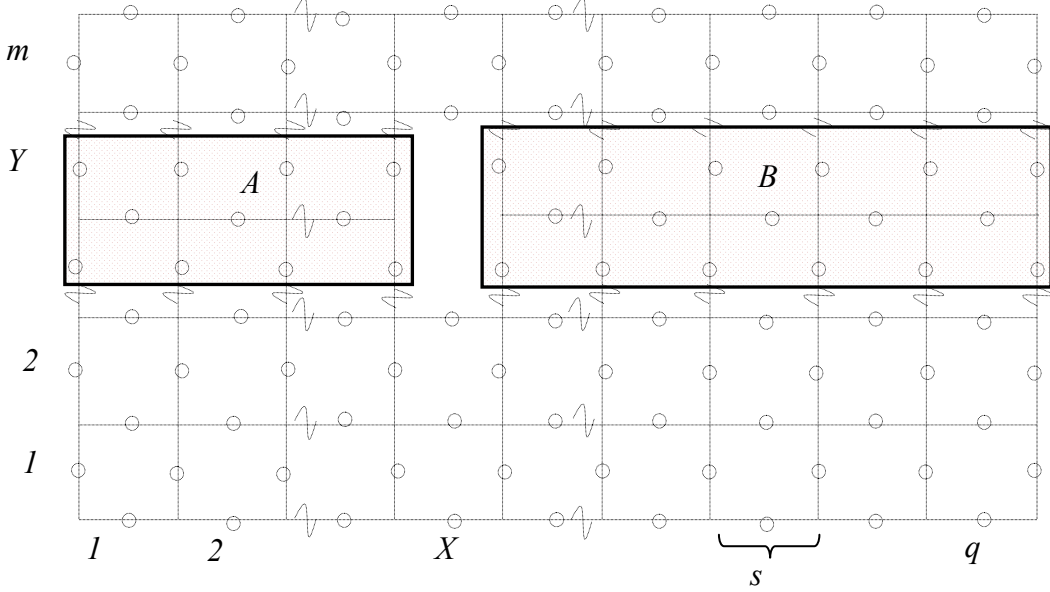


FIGURE 18: Enclosed nodes for computing $R(X,Y)$.

Each of the bottom and uppermost nodes aligned horizontally in region A is at an increased distance of $2s$ with the nodes in region B after the link removal. Thus, there is an overall increase of total distance of $2X \{(2s)(q-X) + s\}$. For the middle layer of nodes, we have a total increase of s , $2s$, and s with the top, middle, and bottom horizontally aligned nodes of region B , respectively. Thus, there is an overall increase of total distance of $(X-1)\{(s+s)(q-X) + 1\} + 2s(q-X)\}$ for the middle horizontally aligned nodes of A . Similarly, we find the total increase in distance of nodes of region B . Using the above discussion, $R_{(X,Y)}$ can be written as:

$$\begin{aligned}
 R_{x,y} &= 2(X)\{2(q-X) + 1\}s + 2(X-1)\{(q-X) + 1\}s + 2(X-1)\{(q-X)\}s \\
 &+ 2(q-x+1)\{2(x-1) + 1\}s + 2(q-x)\{x\}s + 2(q-x)\{x-1\}s \\
 &= 4(4qX - 4X^2 + 4X - 2q - 1)s
 \end{aligned} \tag{25}$$